State-space models for the unsteady lift force due to agile maneuvers and gusts

Steve Brunton & Clancy Rowley
Princeton University
FAA/JUP January 20, 2011

Motivation

Applications of Unsteady Models

Conventional UAVs (performance/robustness)

Flow control, flight dynamic control

Autopilots / Flight simulators

Gust disturbance mitigation

Predator (General Atomics)

FLYIT Simulators, Inc.

Need for State-Space Models

Need models suitable for control

Combining with flight models

Wake Vortex

Shadow (Aerocam)

NextGen ConOps V2.0: UAVs

2.7.2.2 Unmanned Aircraft Systems

UAS operations are some of the most demanding operations in NextGen. UAS operations include scheduled and on-demand flights for a variety of civil, military, and state missions.

Because of the range of operational uses, UAS operators may require access to all NextGen airspace. ...

2.7.2.3 Vertical Flight

... Rotorcraft are also used for UAS applications for commercial, police, and security operations. These operations add to the density and complexity of operations, particularly in and around urban areas.

3.3.1.2.3 Integrated Environmental Operations

UAS performing security functions and the airport perimeter security intrusion detection system may have the capability to assist with wildlife management programs.

5.3.3 Weather Information Enterprise Services

- **Enterprise Service 3:** UASs Are Used for Weather Reconnaissance. [R-169]

En route weather reconnaissance UASs are equipped to collect and report in-flight weather data. Specialized weather reconnaissance UASs are used to scout potential flight routes and trajectories to identify available "weather-favorable" airspace...

Microburst Windshear

Navigating a microburst requires counterintuitive piloting

M.L. Psiaki and R.F. Stengel, *J. Aircraft*: vol. 23, no. 8, 1986.

S.S. Mulgund and R.F. Stengel, *J. Guidance*: vol. 16, no. 6, 1993.

D.A. Stratton and R.F. Stengel, *J. Guidance*: vol. 15, no. 5, 1992.

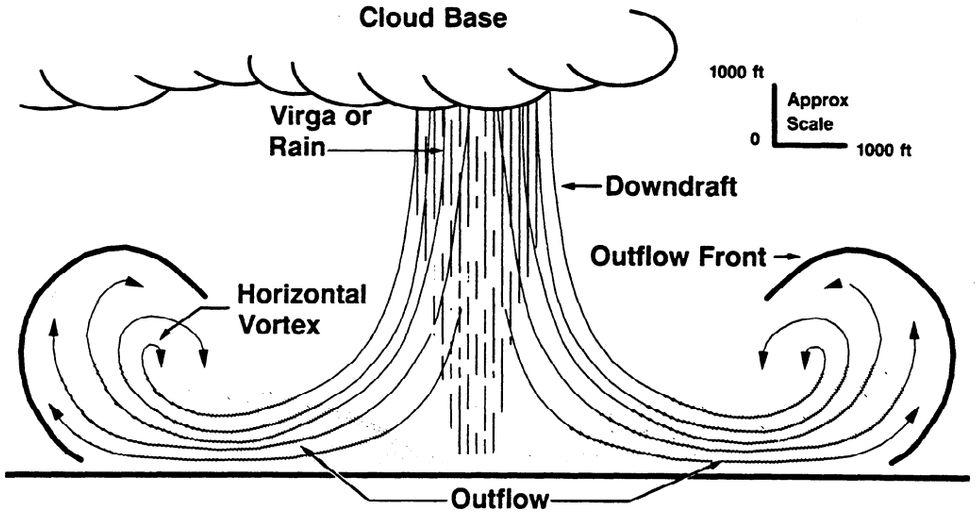

Figure 7. Symmetric microburst. An airplane transiting the microburst would experience equal headwinds and tailwinds.

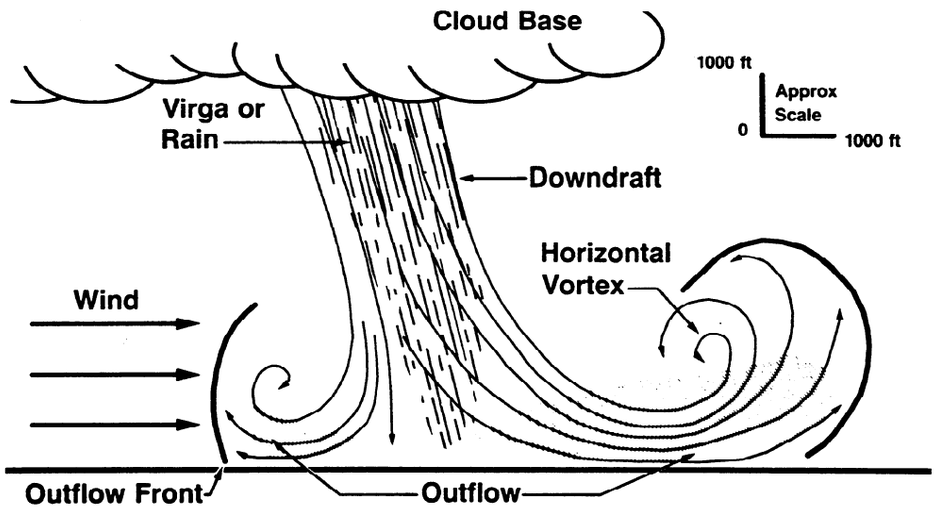

Figure 8. Asymmetric microburst. An airplane transiting the microburst from left to right would experience a small headwind followed by a large tailwind.

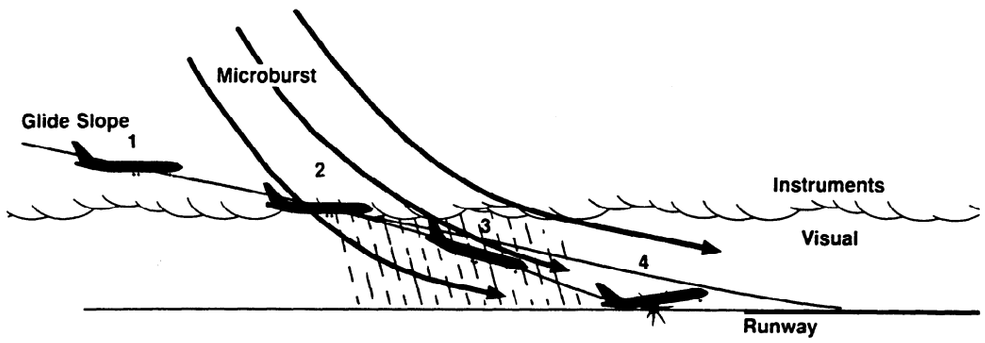

Figure 20. Windshear encounter during approach. (1) Approach initially appeared normal. (2) Increasing downdraft and tailwind encountered at transition. (3) Airspeed decrease combined with reduced visual cues resulted in pitch attitude reduction. (4) Airplane crashed short of approach end of runway.

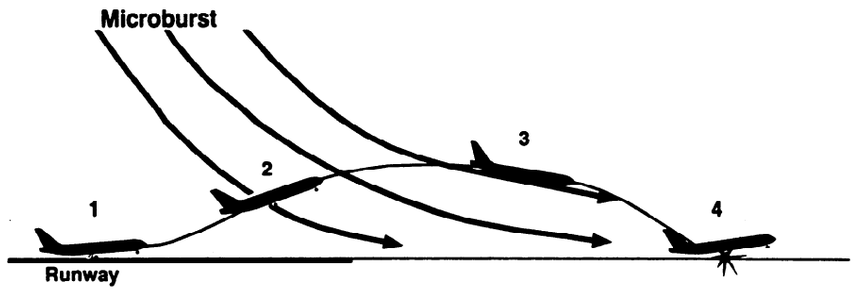

Figure 13. Windshear encounter during takeoff after liftoff. (1) Takeoff initially appeared normal. (2) Windshear encountered just after liftoff. (3) Airspeed decrease resulted in pitch attitude reduction. (4) Aircraft crashed off departure end of runway 20 sec after liftoff.

Stall velocity and size

Smaller, lower stall velocity

RQ-1 Predator
(27 m/s stall)

Daedalus Dakota
(18m/s stall)

Puma AE
(10 m/s stall)

$$V_{\text{stall}} = \sqrt{\frac{2}{\rho}\left(C_{L_{\max}} S\right)^{-1} W}$$

S	Wing surface area
W	Aircraft weight
L	Lift force
C_L	Lift coefficient
V	Velocity of aircraft

UAV Flight Envelope

1. ***Landing approach speed is 30% higher than stall speed***

2. ***$C_{L_{\max}}$ occurs at the stall speed V_{stall}***

$$V_{\text{stall}} = \sqrt{\frac{2}{\rho}\left(C_{L_{\max}} S\right)^{-1} W}$$

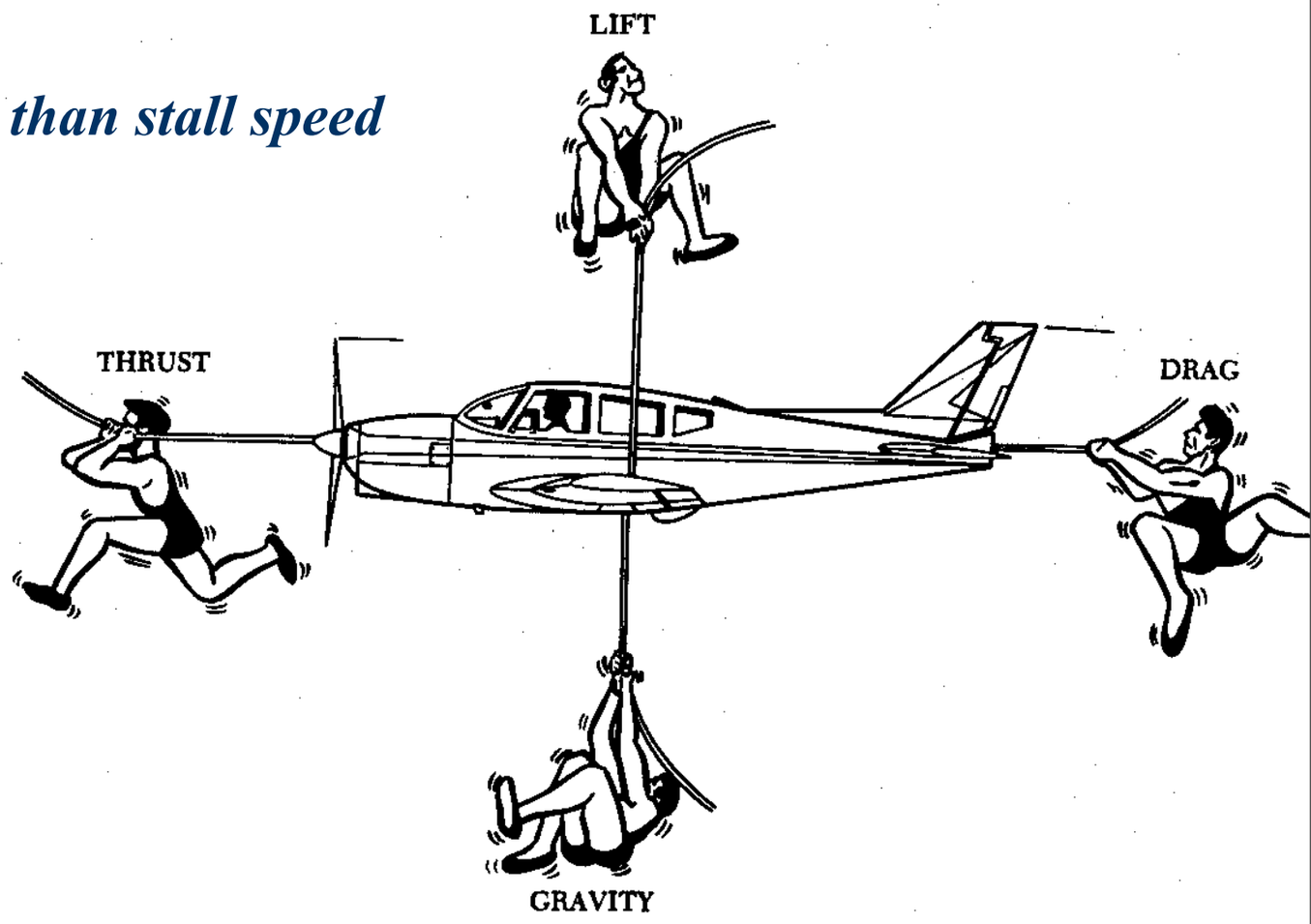

FIGURE 2–7. Forces in action in flight.

i.e.

$$W = L_{\max} = C_{L_{\max}} \bar{q} S = C_{L_{\max}} \cdot \left(\frac{1}{2}\rho V_{\text{stall}}^2\right) \cdot S$$

S	**Wing surface area**
W	**Aircraft weight**
L	**Lift force**
C_L	**Lift coefficient**
V	**Velocity of aircraft**

$$C_{L_{\max}} \in [1, 1.5]$$

for reasonable aspect ratio

3 Types of Unsteadiness

1. High angle-of-attack

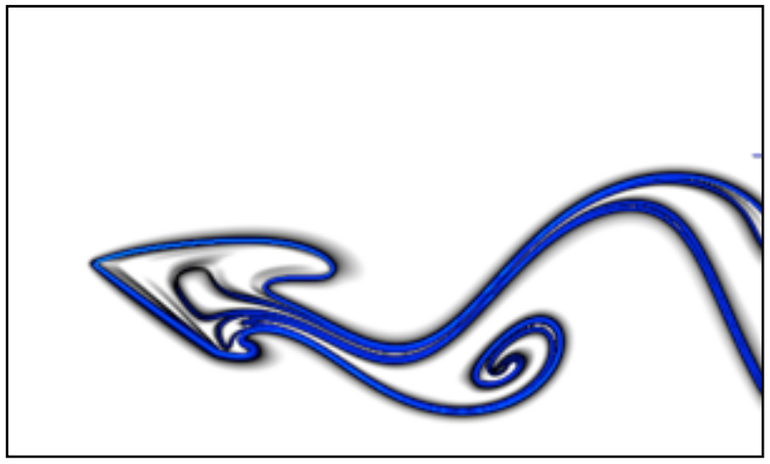

$$\alpha > \alpha_{\text{stall}}$$

Large amplitude, slow

2. Strouhal number

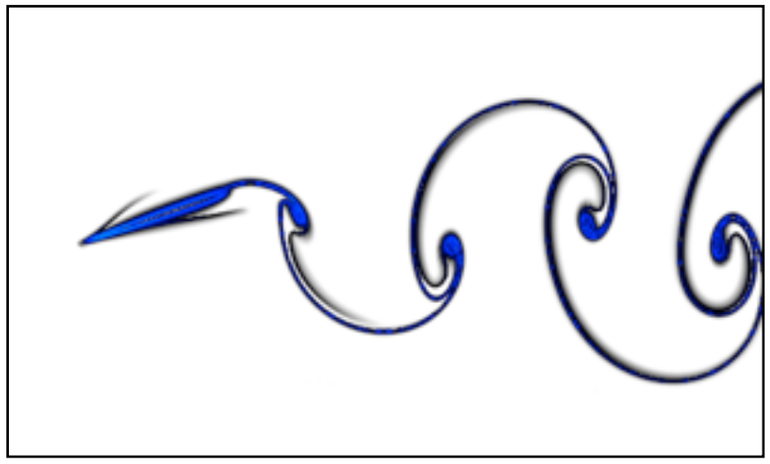

$$St = \frac{Af}{U_\infty}$$

Moderate amplitude, fast

3. Reduced frequency

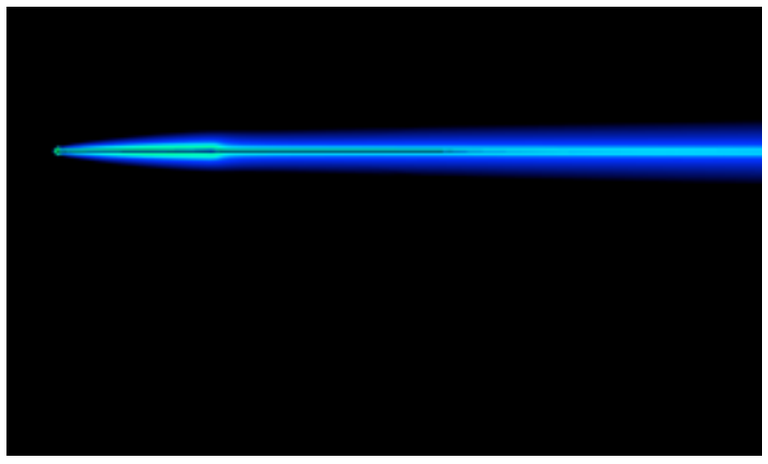

$$k = \frac{\pi f c}{U_\infty}$$

Small amplitude, very fast

Closely related

$$\alpha_{\text{eff}} = \tan^{-1}(\pi St)$$

Brunton and Rowley, AIAA ASM 2009

3 Types of Unsteadiness

1. High angle-of-attack

$$\alpha > \alpha_{\text{stall}}$$

Large amplitude, slow

2. Strouhal number

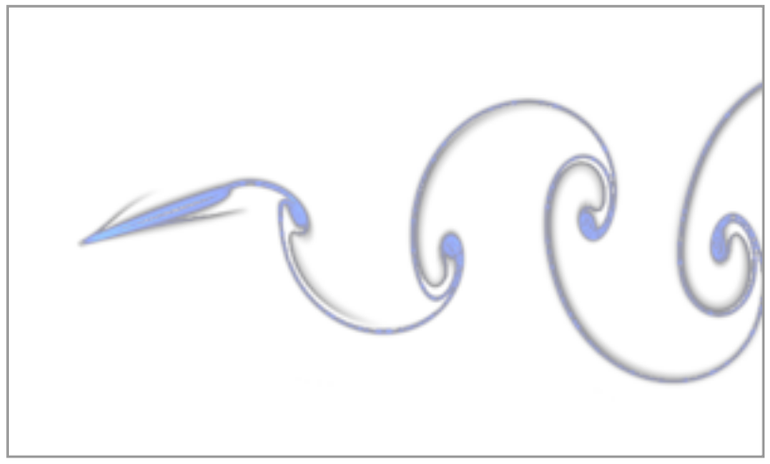

$$St = \frac{Af}{U_\infty}$$

Moderate amplitude, fast

3. Reduced frequency

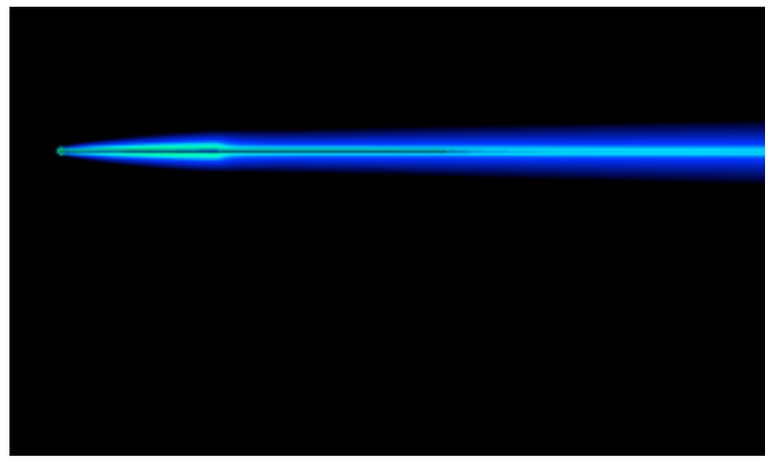

$$k = \frac{\pi f c}{U_\infty}$$

Small amplitude, very fast

(flutter instability, fast gust disturbance, rapid maneuver)

Closely related

$$\alpha_{\text{eff}} = \tan^{-1}(\pi St)$$

Brunton and Rowley, AIAA ASM 2009

Coupled Flight Dynamic Model

coupled model

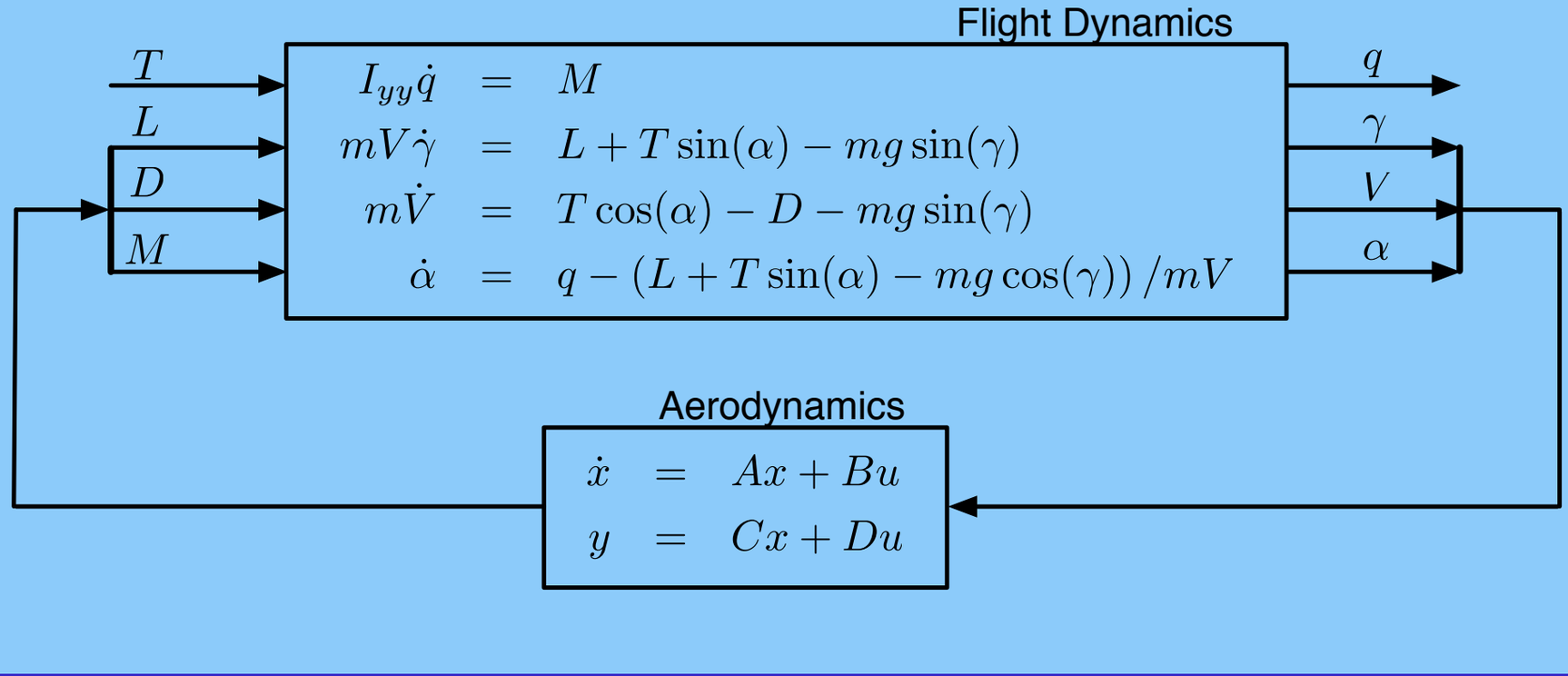

Interesting control scenario when time-scales of flight dynamics are close to time-scales of aerodynamics

Candidate Lift Models

$$C_L = 2\pi\alpha$$

$$C_L = C_{L_\alpha}\alpha$$

$$C_L = C_L(\alpha)$$

$$C_L(t) = C_L^\delta(t)\alpha(0) + \int_0^t C_L^\delta(t-\tau)\dot{\alpha}(\tau)d\tau$$

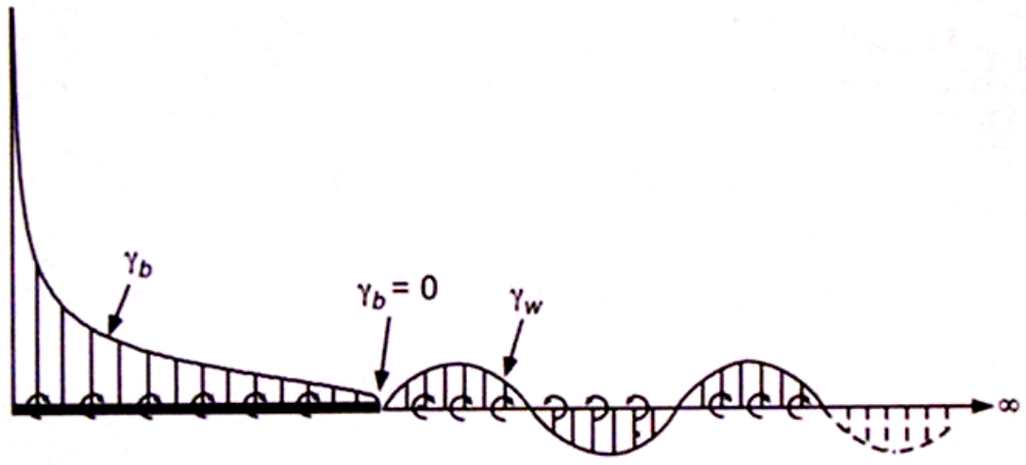

Wagner's Indicial Response

$$C_L = \underbrace{\frac{\pi}{2}\left[\ddot{h} + \dot{\alpha} - \frac{a}{2}\ddot{\alpha}\right]}_{\text{Added-Mass}} + \underbrace{2\pi\left[\alpha + \dot{h} + \frac{1}{2}\dot{\alpha}\left(\frac{1}{2} - a\right)\right]}_{\text{Circulatory}} C(k)$$

Theodorsen's Model

Motivation for State-Space Models

Captures input output dynamics accurately

Computationally tractable

fits into control framework

Wagner, 1925.

Theodorsen, 1935.

Leishman, 2006.

Lift vs. Angle of Attack

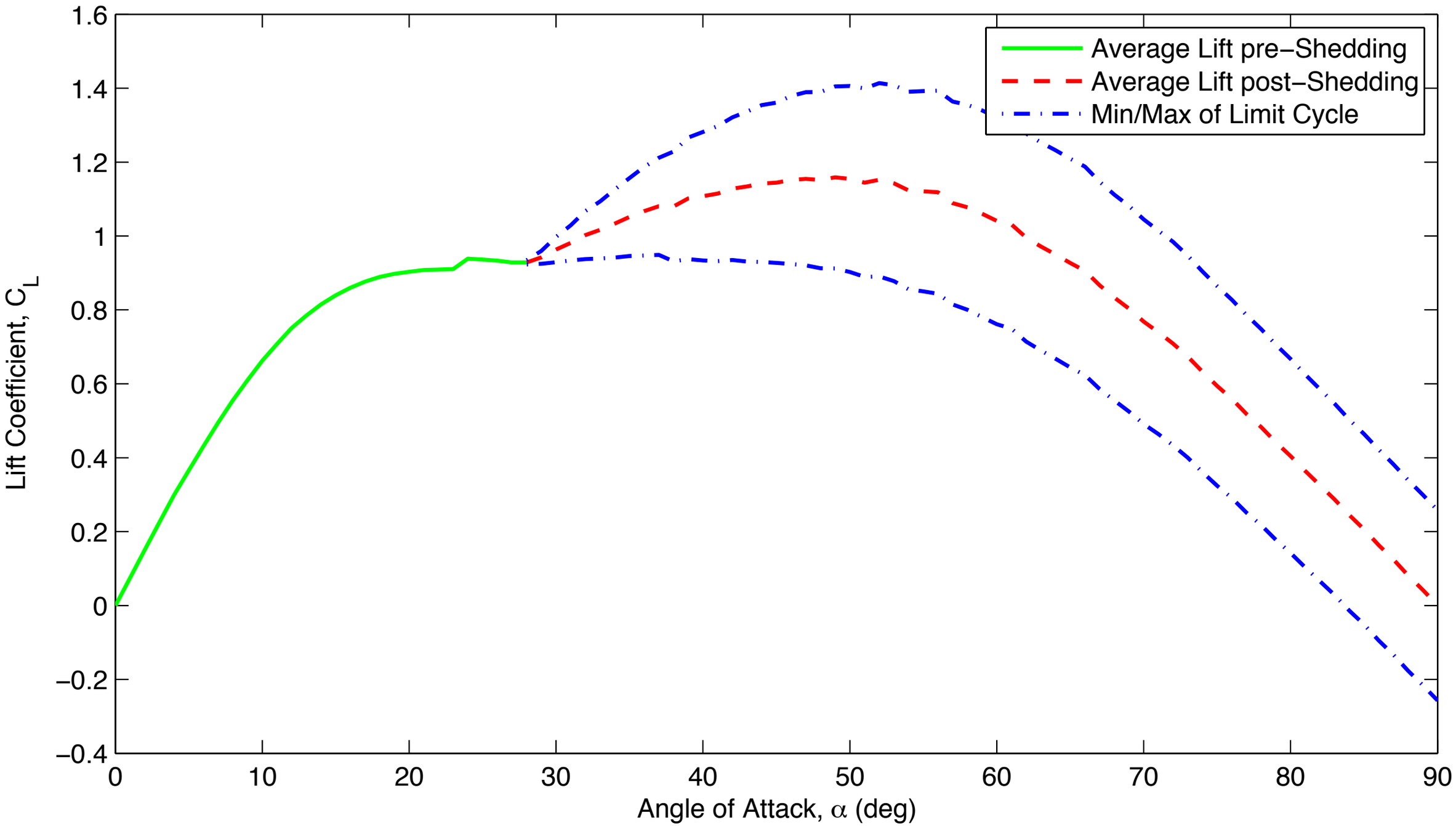

Low Reynolds number, (Re=100)

Hopf bifurcation at $\alpha_{\text{crit}} \approx 28^\circ$ **(pair of imaginary eigenvalues pass into right half plane)**

Lift vs. Angle of Attack

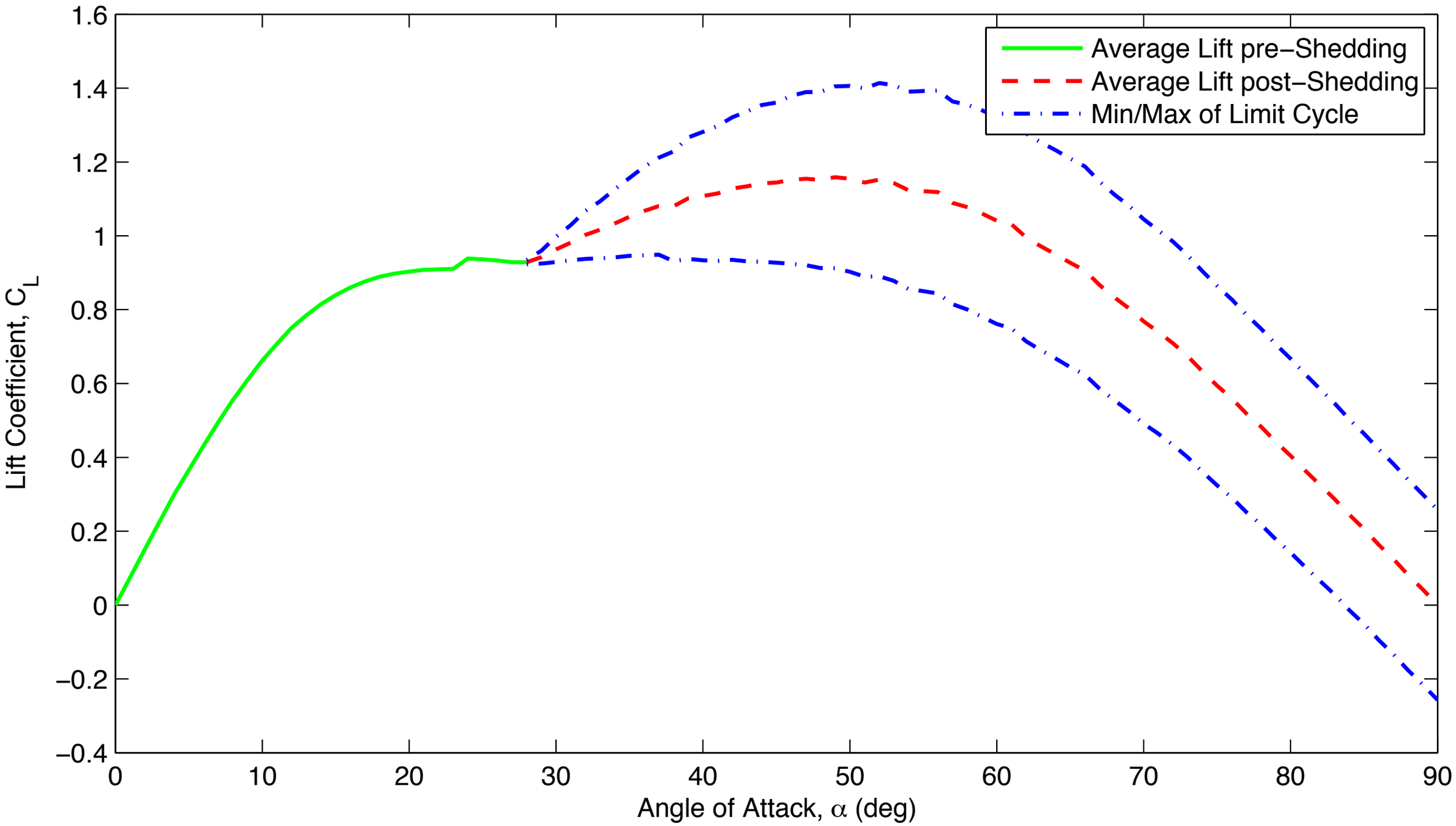

Need model that captures lift due to moving airfoil!

Lift vs. Angle of Attack

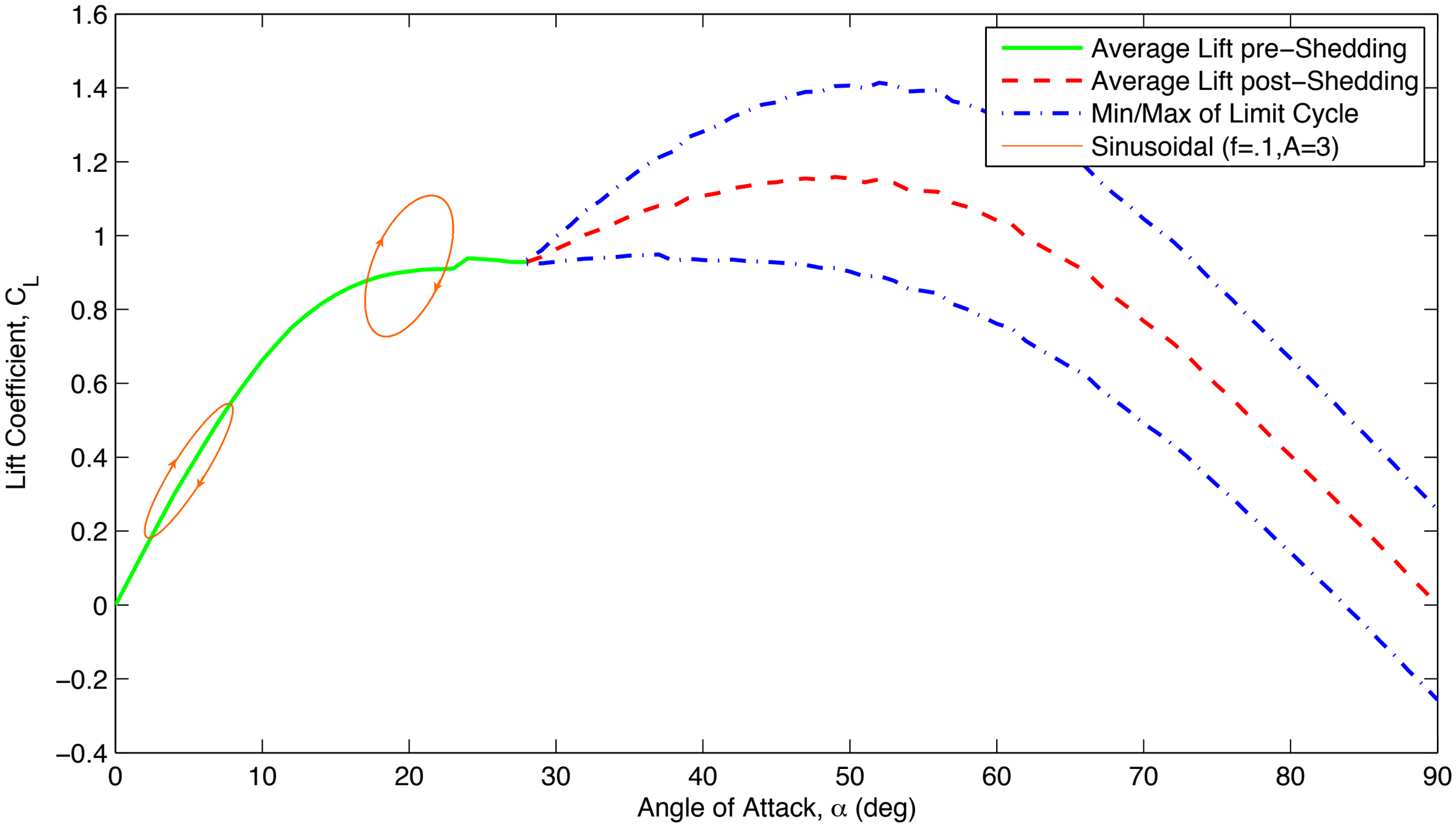

Need model that captures lift due to moving airfoil!

Lift vs. Angle of Attack

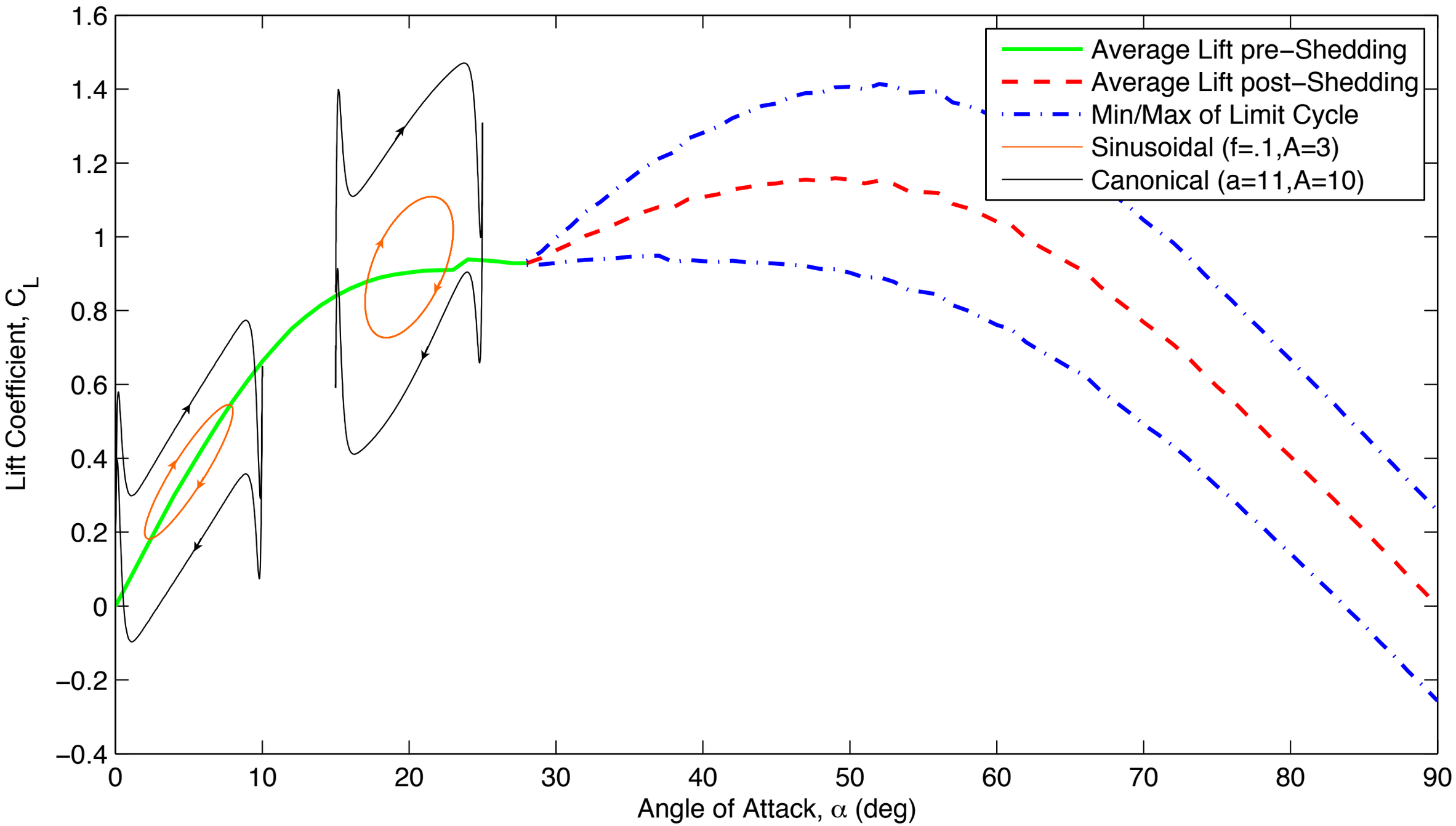

Need model that captures lift due to moving airfoil!

Lift vs. Angle of Attack

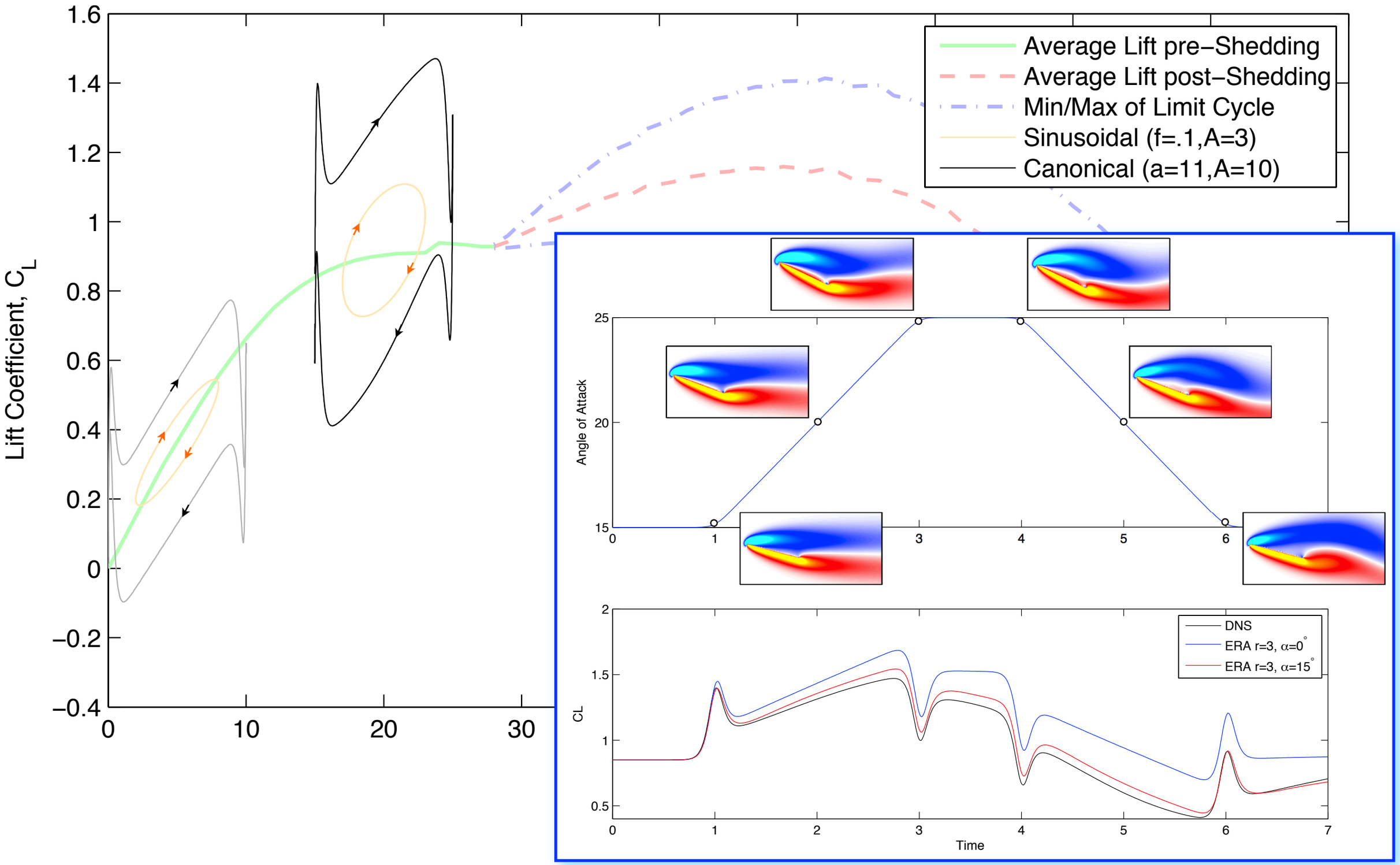

Need model that captures lift due to moving airfoil!

Lift vs. Angle of Attack

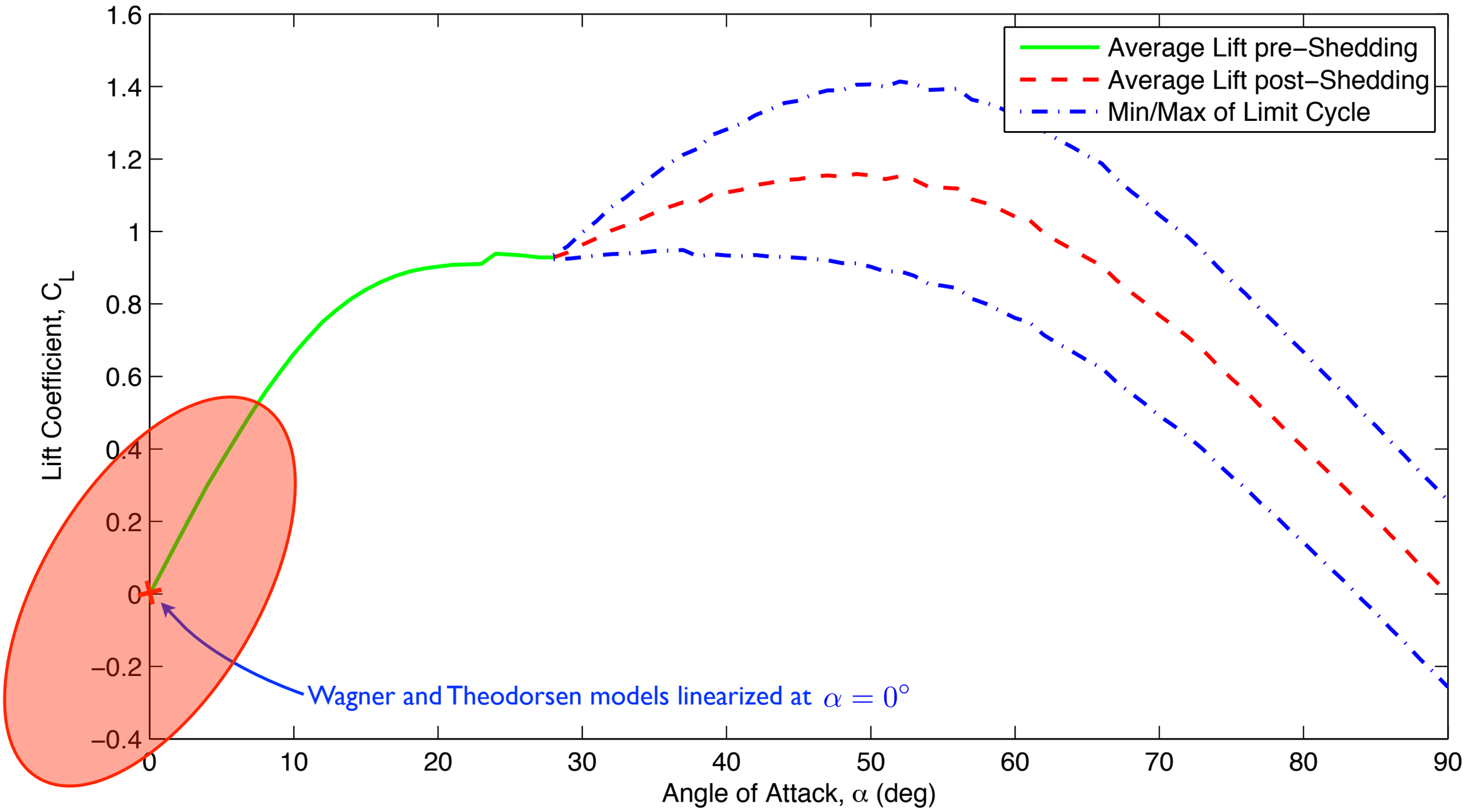

Theodorsen's Model

$$C_L = \underbrace{\frac{\pi}{2}\left[\ddot{h} + \dot{\alpha} - \frac{a}{2}\ddot{\alpha}\right]}_{\text{Added-Mass}} + \underbrace{2\pi\left[\alpha + \dot{h} + \frac{1}{2}\dot{\alpha}\left(\frac{1}{2} - a\right)\right]}_{\text{Circulatory}} C(k)$$

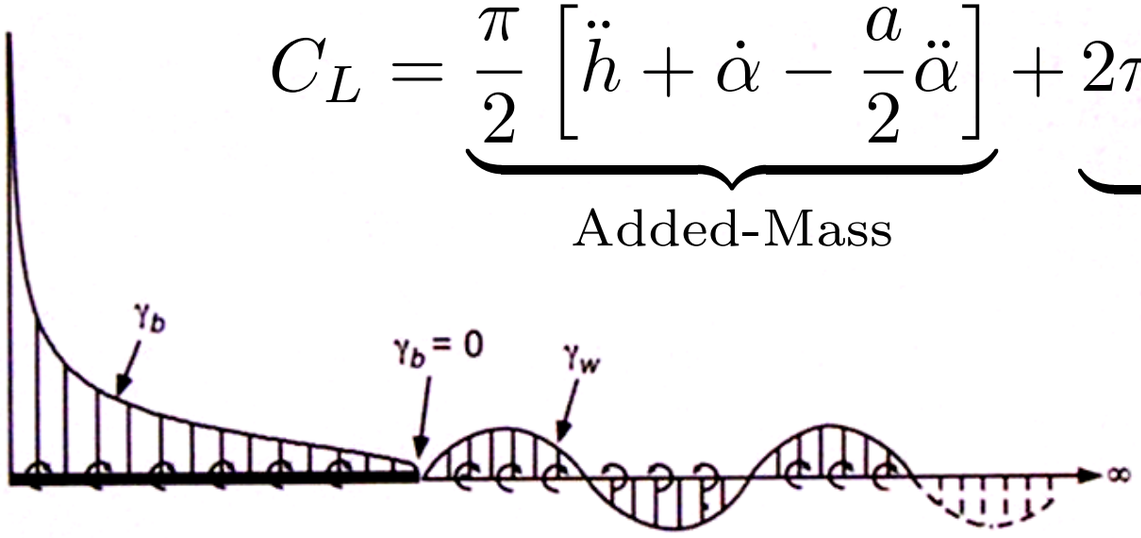

$$C(k) = \frac{H_1^{(2)}(k)}{H_1^{(2)}(k) + iH_0^{(2)}(k)}$$

2D Incompressible, inviscid model

Unsteady potential flow (w/ Kutta condition)

Linearized about zero angle of attack

$$k = \frac{\pi f c}{U_\infty}$$

Apparent Mass

Increasingly important for lighter aircraft

Not trivial to compute, but essentially solved

force needed to move air as plate accelerates

Circulatory Lift

Captures separation effects

Need improved models here

source of all lift in steady flight

Theodorsen, 1935.

Leishman, 2006.

Empirical Theodorsen

$$C_L = \underbrace{\frac{\pi}{2}\left[\ddot{h} + \dot{\alpha} - \frac{a}{2}\ddot{\alpha}\right]}_{\text{Added-Mass}} + \underbrace{2\pi\left[\alpha + \dot{h} + \frac{1}{2}\dot{\alpha}\left(\frac{1}{2} - a\right)\right]}_{\text{Circulatory}} C(k)$$

Generalized Coefficients

$$C_L = C_1\left[\dot{\alpha} - \frac{a}{2}\ddot{\alpha}\right] + C_2\left[\alpha + \frac{1}{2}\dot{\alpha}\left(\frac{1}{2} - a\right)\right] C(k)$$

Transfer Function

$$\frac{\mathcal{L}\left[C_L\right]}{\mathcal{L}\left[\ddot{\alpha}\right]} = C_1\left(\frac{1}{s} - \frac{a}{2}\right) + C_2\left[\frac{1}{s^2} + \frac{1}{2s}\left(\frac{1}{2} - a\right)\right] C(s)$$

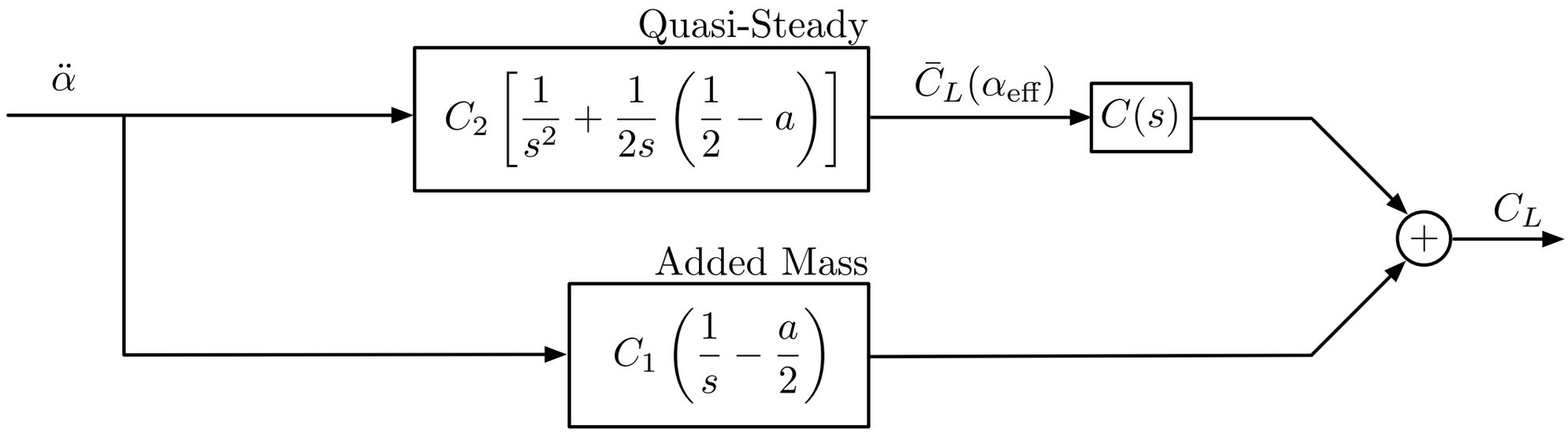

Wagner's Indicial Response

Given an impulse in angle of attack, $\alpha = \delta(t)$, the time history of Lift is $C_L^\delta(t)$

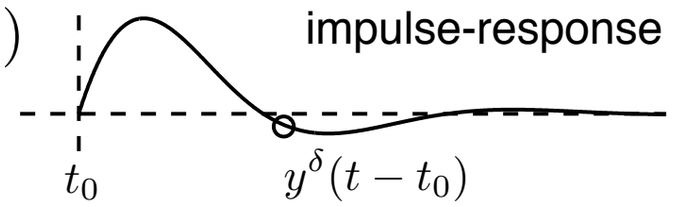

The response to an arbitrary input $\alpha(t)$ is given by linear superposition:

$$C_L(t) = \int_0^t C_L^\delta(t-\tau)\alpha(\tau)d\tau = \left(C_L^\delta * \alpha\right)(t)$$

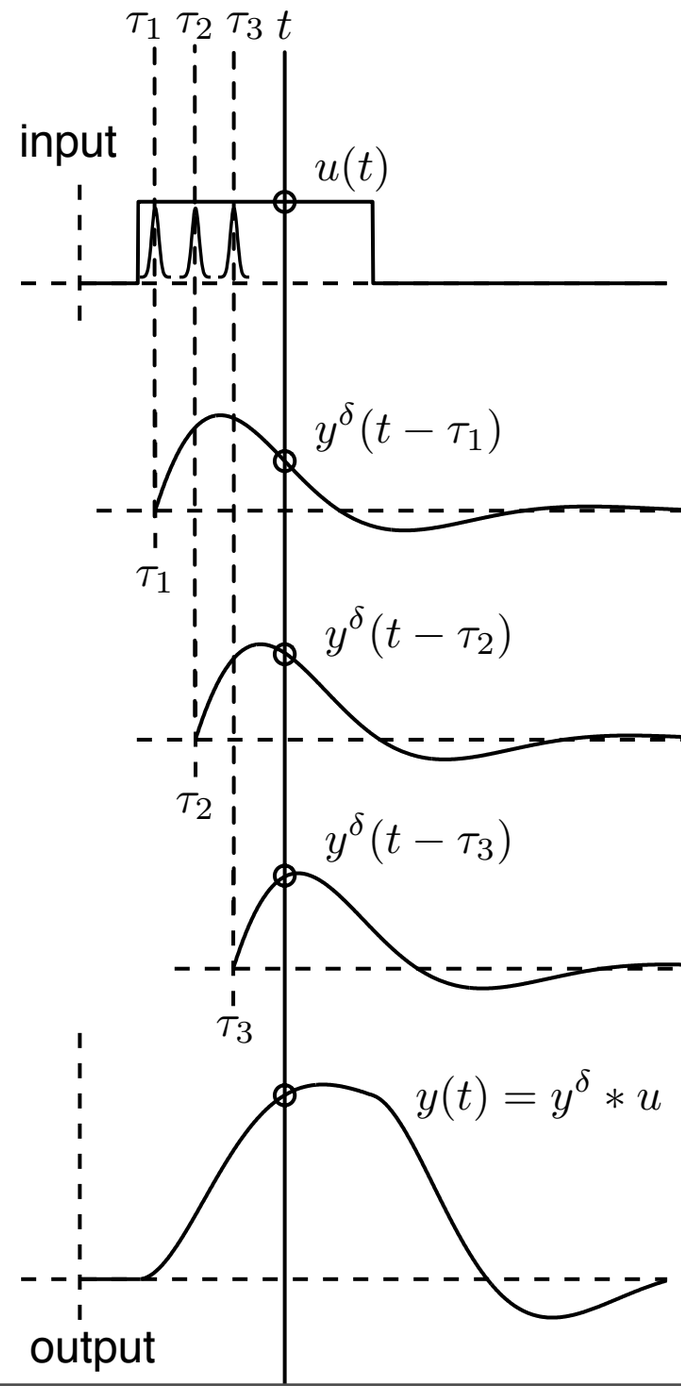

Given a step in angle of attack, $\dot{\alpha} = \delta(t)$, the time history of Lift is $C_L^S(t)$

The response to an arbitrary input $\alpha(t)$ is given by:

$$C_L(t) = C_L^S(t)\alpha(0) + \int_0^t C_L^S(t-\tau)\dot{\alpha}(\tau)d\tau$$

Model Summary

Reconstructs Lift for arbitrary input

Linearized about $\alpha = 0$

Based on experiment, simulation or theory

convolution integral inconvenient for feedback control design

Wagner, 1925.

Leishman, 2006.

Reduced Order Wagner

Stability derivatives plus fast dynamics

$$C_L(\alpha, \dot{\alpha}, \ddot{\alpha}, \mathbf{x}) = C_{L_\alpha}\alpha + C_{L_{\dot{\alpha}}}\dot{\alpha} + C_{L_{\ddot{\alpha}}}\ddot{\alpha} + C\mathbf{x}$$

Quasi-steady and added-mass

Fast dynamics

Transfer Function

$$Y(s) = \left[\frac{C_{L_\alpha}}{s^2} + \frac{C_{L_{\dot{\alpha}}}}{s} + C_{L_{\ddot{\alpha}}} + G(s)\right] s^2 U(s)$$

State-Space Form

$$\frac{d}{dt}\begin{bmatrix}\mathbf{x}\\ \alpha\\ \dot{\alpha}\end{bmatrix} = \begin{bmatrix}A_r & 0 & 0\\ 0 & 0 & 1\\ 0 & 0 & 0\end{bmatrix}\begin{bmatrix}\mathbf{x}\\ \alpha\\ \dot{\alpha}\end{bmatrix} + \begin{bmatrix}B_r\\ 0\\ 1\end{bmatrix}\ddot{\alpha}$$

$$C_L = \begin{bmatrix}C_r & C_{L_\alpha} & C_{L_{\dot{\alpha}}}\end{bmatrix}\begin{bmatrix}\mathbf{x}\\ \alpha\\ \dot{\alpha}\end{bmatrix} + C_{L_{\ddot{\alpha}}}\ddot{\alpha}$$

Reduced Order Wagner

$$C_L(t) = C_L^S(t)\alpha(0) + \int_0^t C_L^S(t-\tau)\dot{\alpha}(\tau)d\tau$$

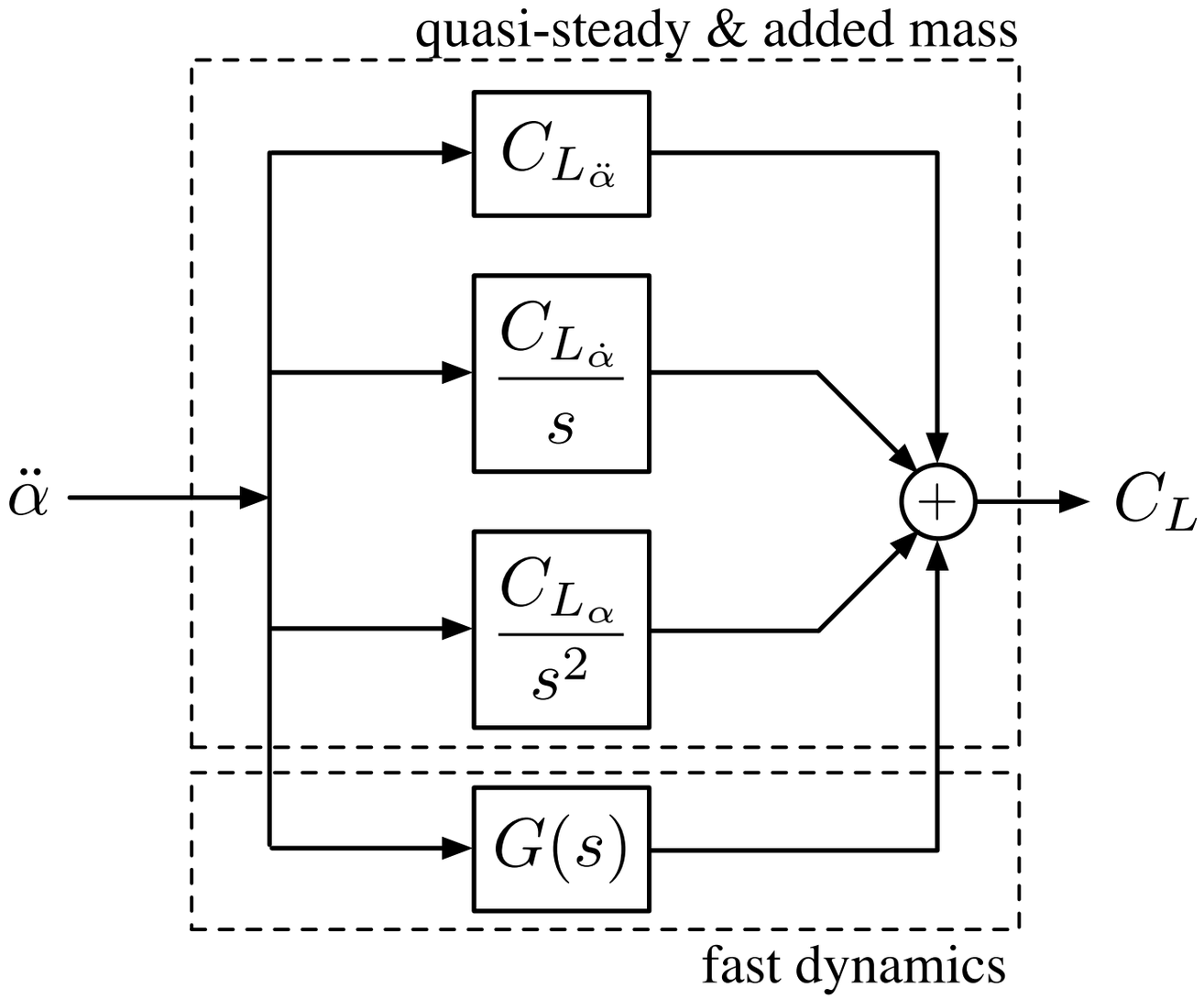

fast dynamics

$$\frac{d}{dt}\begin{bmatrix}\mathbf{x}\\ \alpha\\ \dot{\alpha}\end{bmatrix} = \begin{bmatrix}A_r & 0 & 0\\ 0 & 0 & 1\\ 0 & 0 & 0\end{bmatrix}\begin{bmatrix}\mathbf{x}\\ \alpha\\ \dot{\alpha}\end{bmatrix} + \begin{bmatrix}B_r\\ 0\\ 1\end{bmatrix}\ddot{\alpha}$$

input

$$C_L = \begin{bmatrix}C_r & C_{L_\alpha} & C_{L_{\dot{\alpha}}}\end{bmatrix}\begin{bmatrix}\mathbf{x}\\ \alpha\\ \dot{\alpha}\end{bmatrix} + C_{L_{\ddot{\alpha}}}\ddot{\alpha}$$

ERA Model

quasi-steady and added-mass

Model Summary

Linearized about $\alpha = 0$

Based on experiment, simulation or theory

Recovers stability derivatives $C_{L_\alpha}, C_{L_{\dot{\alpha}}}, C_{L_{\ddot{\alpha}}}$ associated with quasi-steady and added-mass

ODE model ideal for control design

Brunton and Rowley, *in preparation*.

Bode Plot - Pitch (LE)

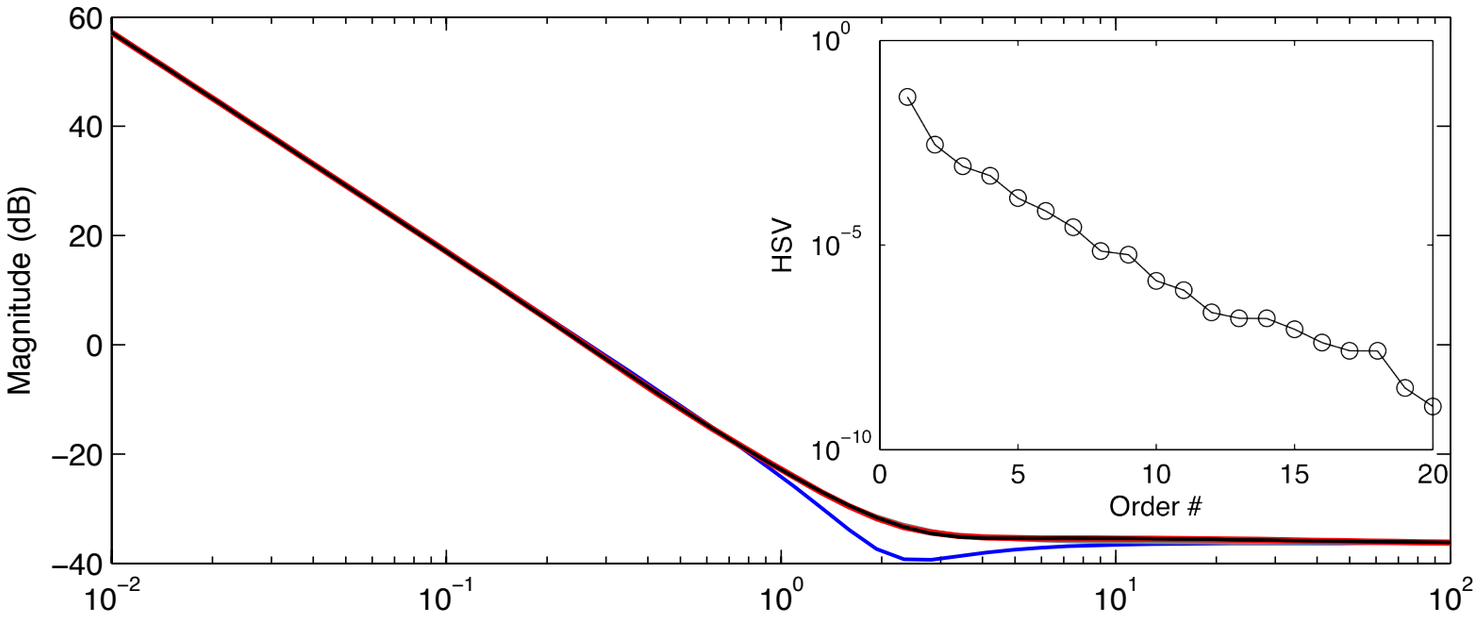

Frequency response

input is $\ddot{\alpha}$ (α is angle of attack)

output is lift coefficient C_L

Pitching at leading edge

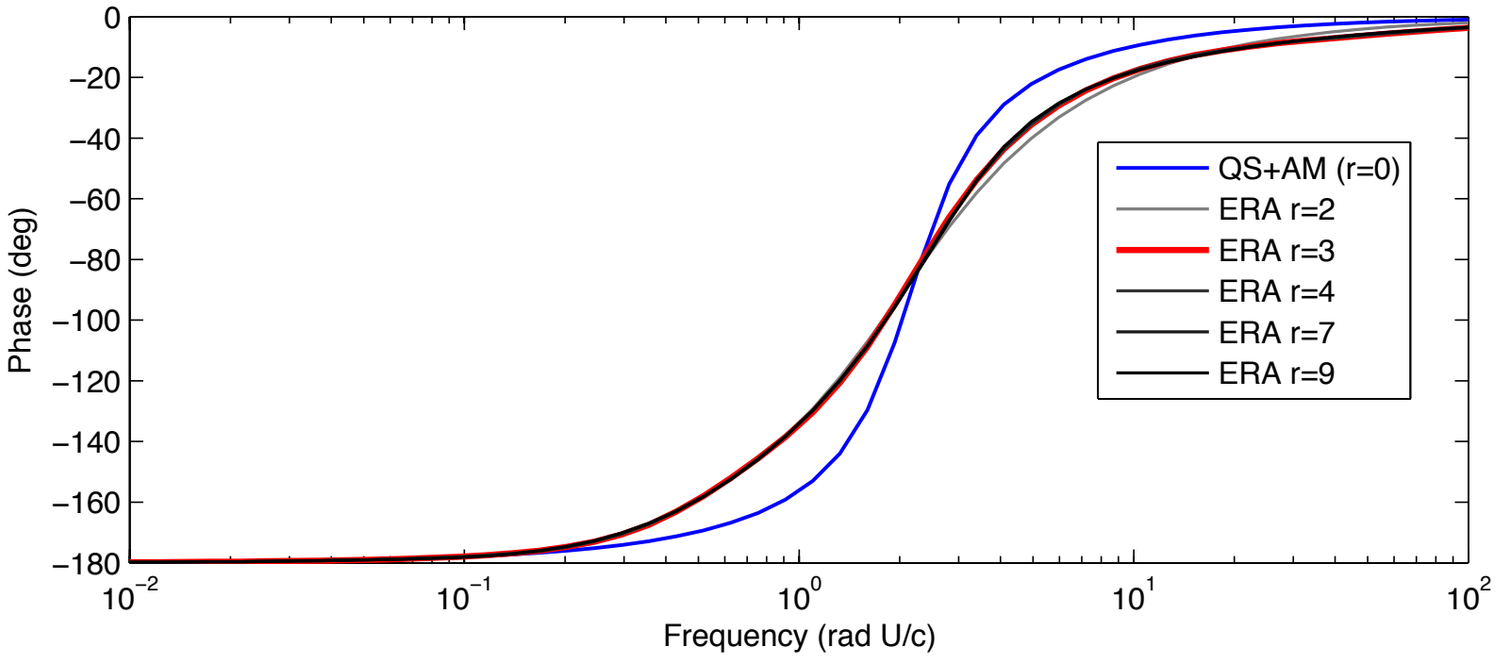

Model without additional fast dynamics [QS+AM (r=0)] is inaccurate in crossover region

Models with fast dynamics of ERA model order >3 are converged

Punchline: additional fast dynamics (ERA model) are essential

Brunton and Rowley, *in preparation*.

Bode Plot - Pitch (QC)

Frequency response

input is $\ddot{\alpha}$ (α is angle of attack)

output is lift coefficient C_L

Pitching at quarter chord

Reduced order model with ERA r=3 accurately reproduces Wagner

Wagner and ROM agree better with DNS than Theodorsen's model.

Asymptotes are correct for Wagner because it is based on experiment

Model for pitch/plunge dynamics [ERA, r=3 (MIMO)] works as well, for the same order model

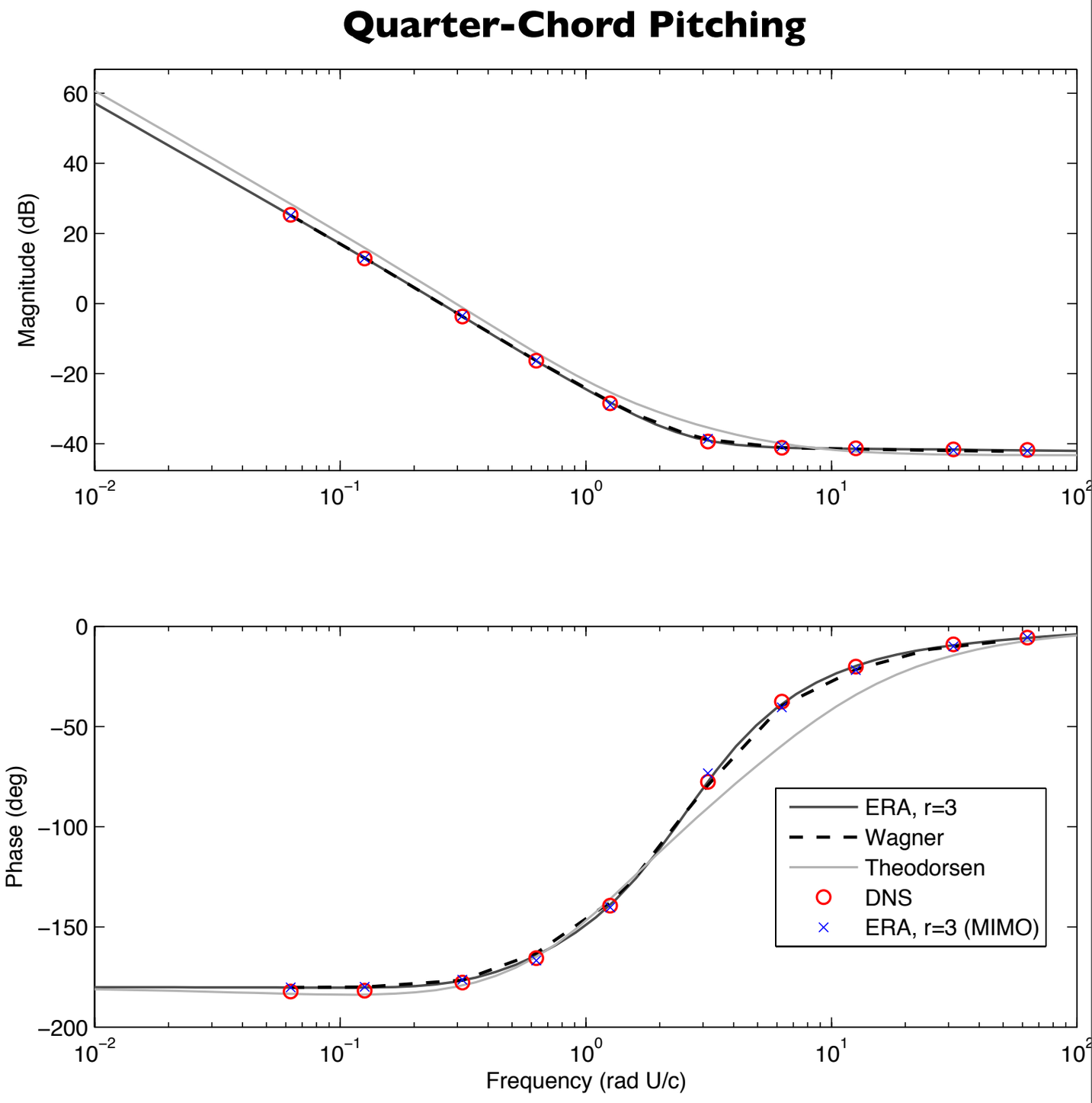

Brunton and Rowley, *in preparation*.

Pitch/Plunge Maneuver

Canonical pitch-up, hold, pitch-down maneuver, followed by step-up in vertical position

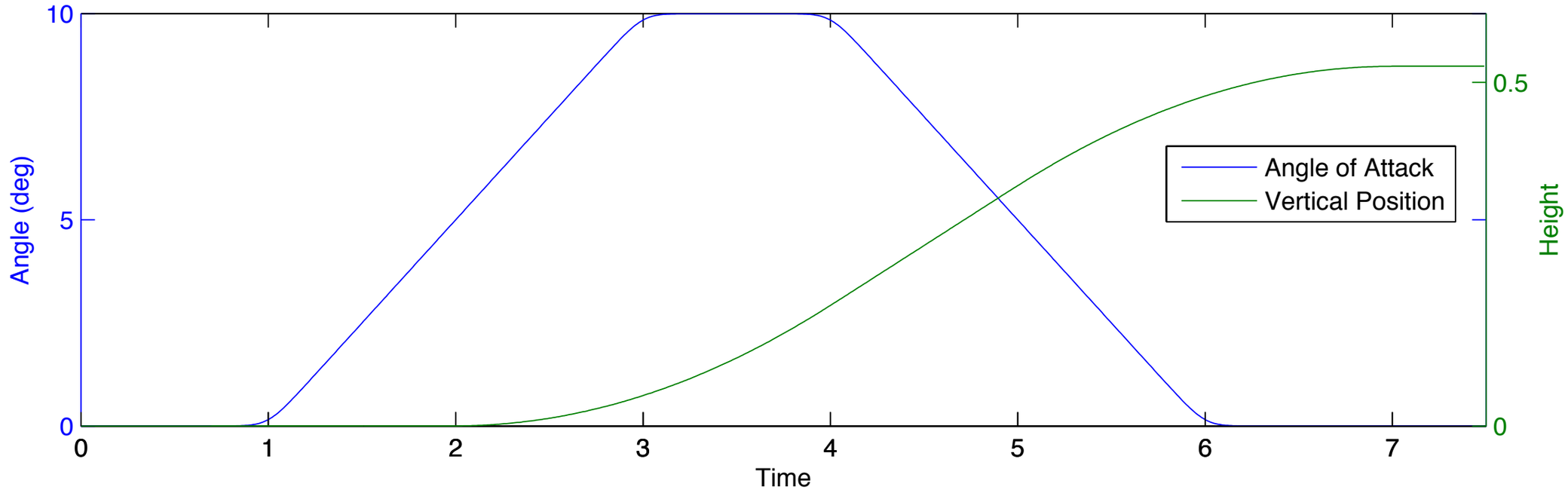

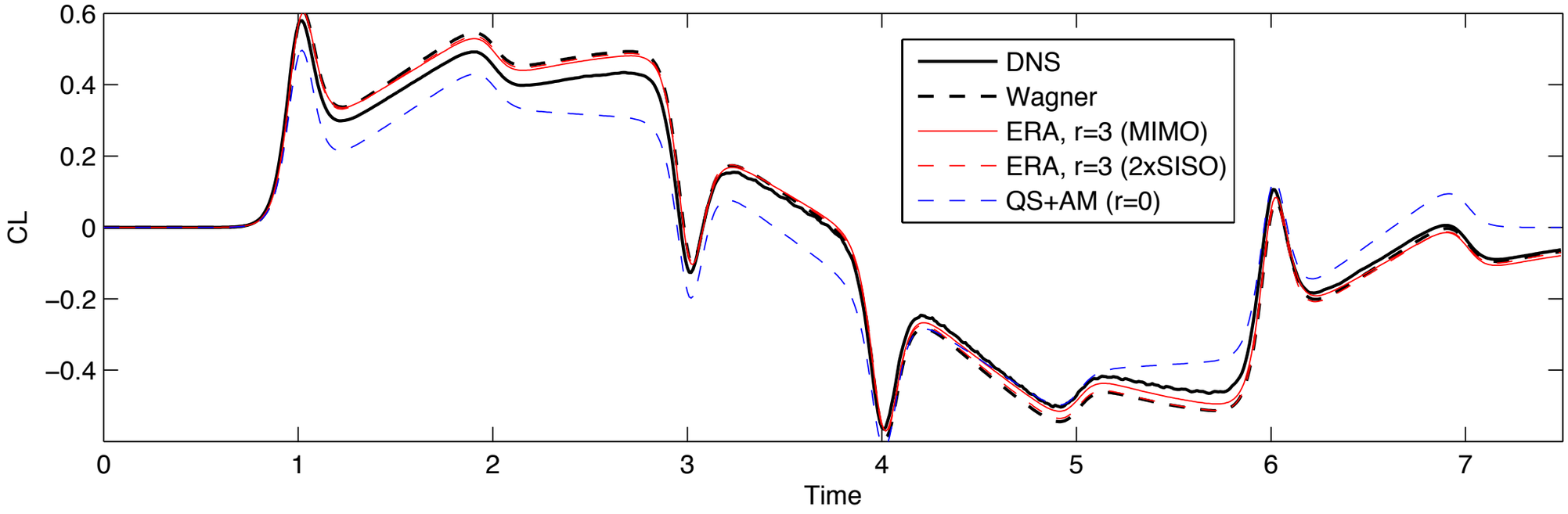

OL, Altman, Eldredge, Garmann, and Lian, 2010

Brunton and Rowley, *in preparation*.

Reduced order model for Wagner's indicial response accurately captures lift coefficient history from DNS

Lift vs. Angle of Attack

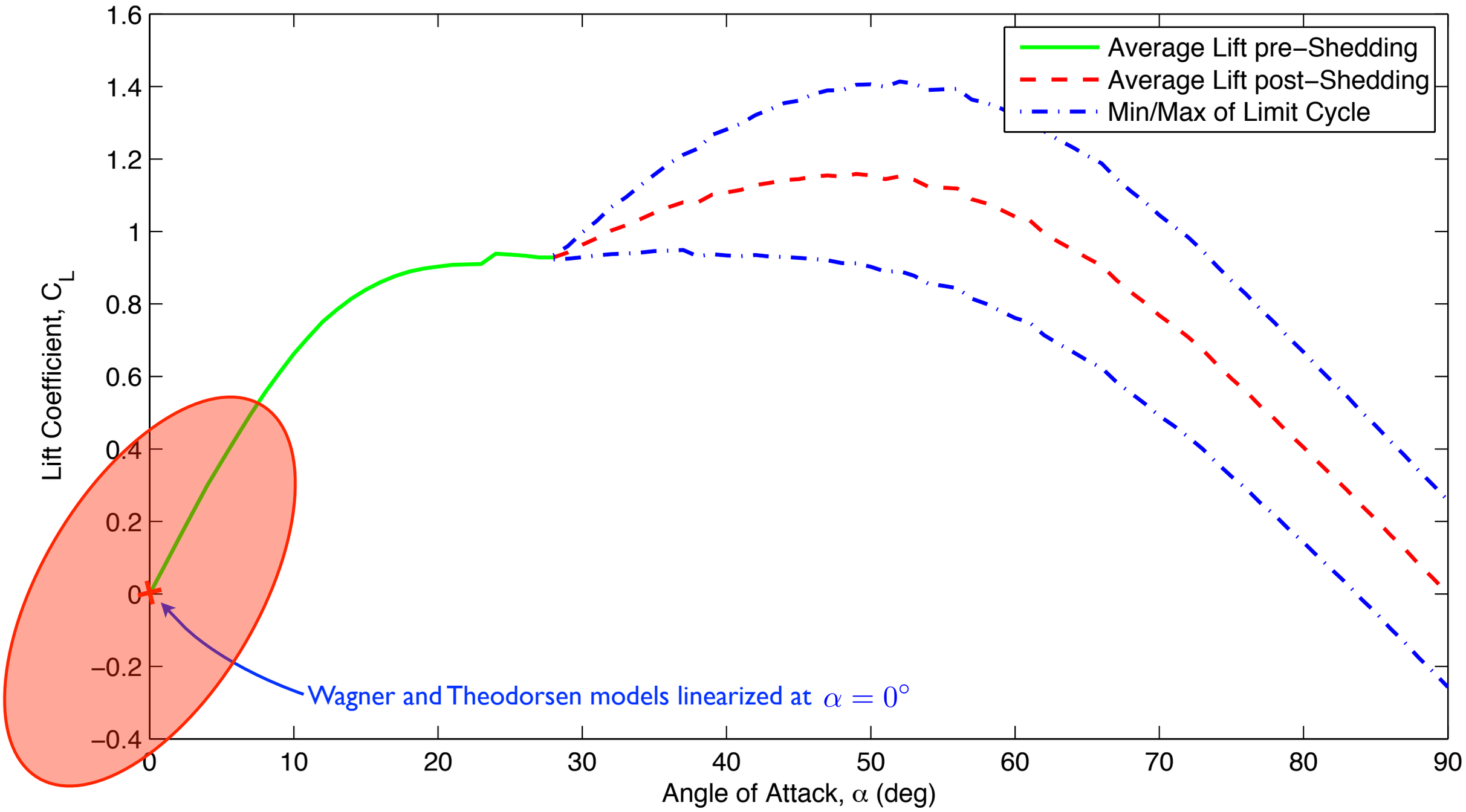

Lift vs. Angle of Attack

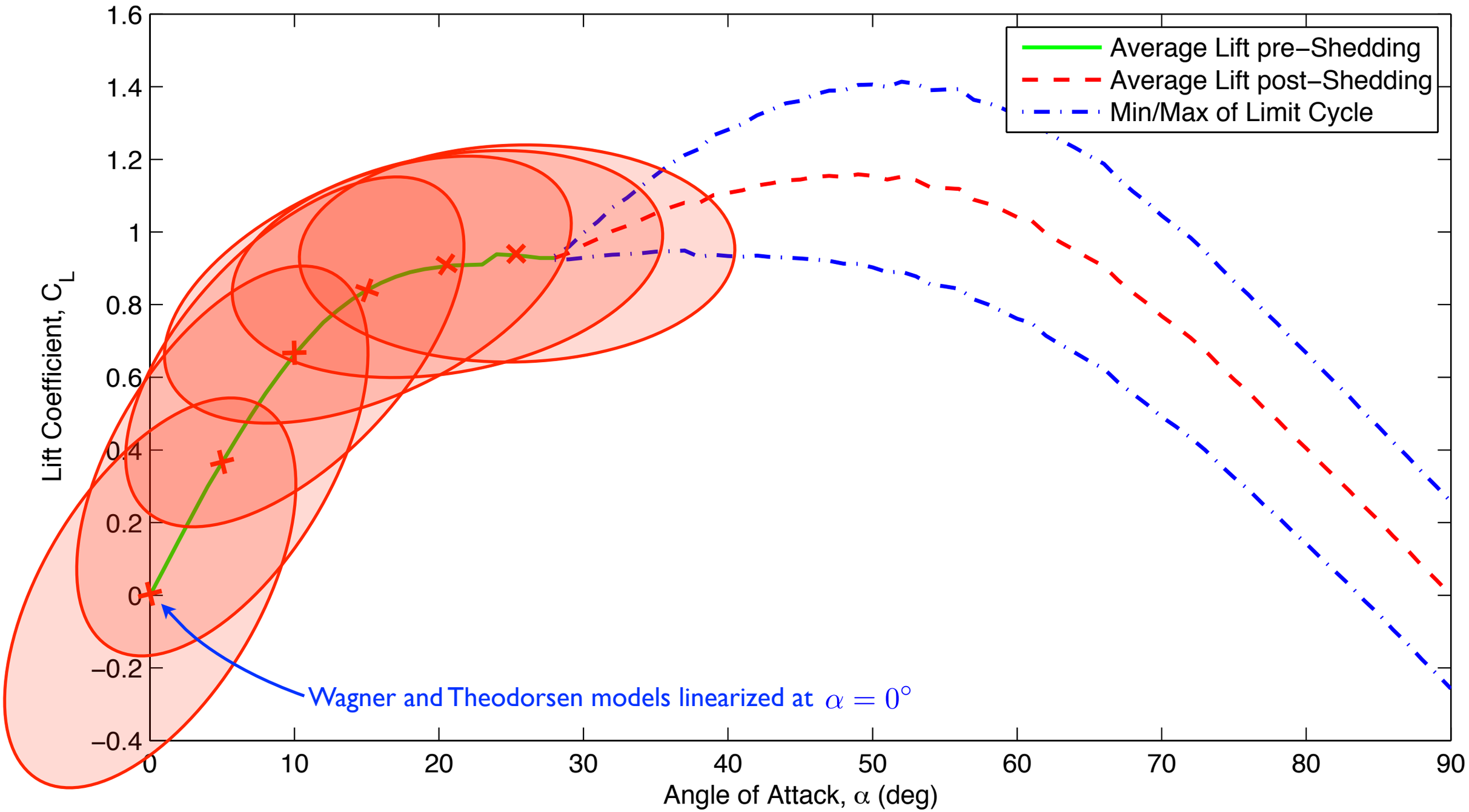

Bode Plot of ERA Models

Results

Lift slope decreases for increasing angle of attack, so magnitude of low frequency motions decreases for increasing angle of attack.

At larger angle of attack, phase converges to -180 at much lower frequencies. I.e., solutions take longer to reach equilibrium in time domain.

Consistent with fact that for large angle of attack, system is closer to Hopf instability, and a pair of eigenvalues are moving closer to imaginary axis.

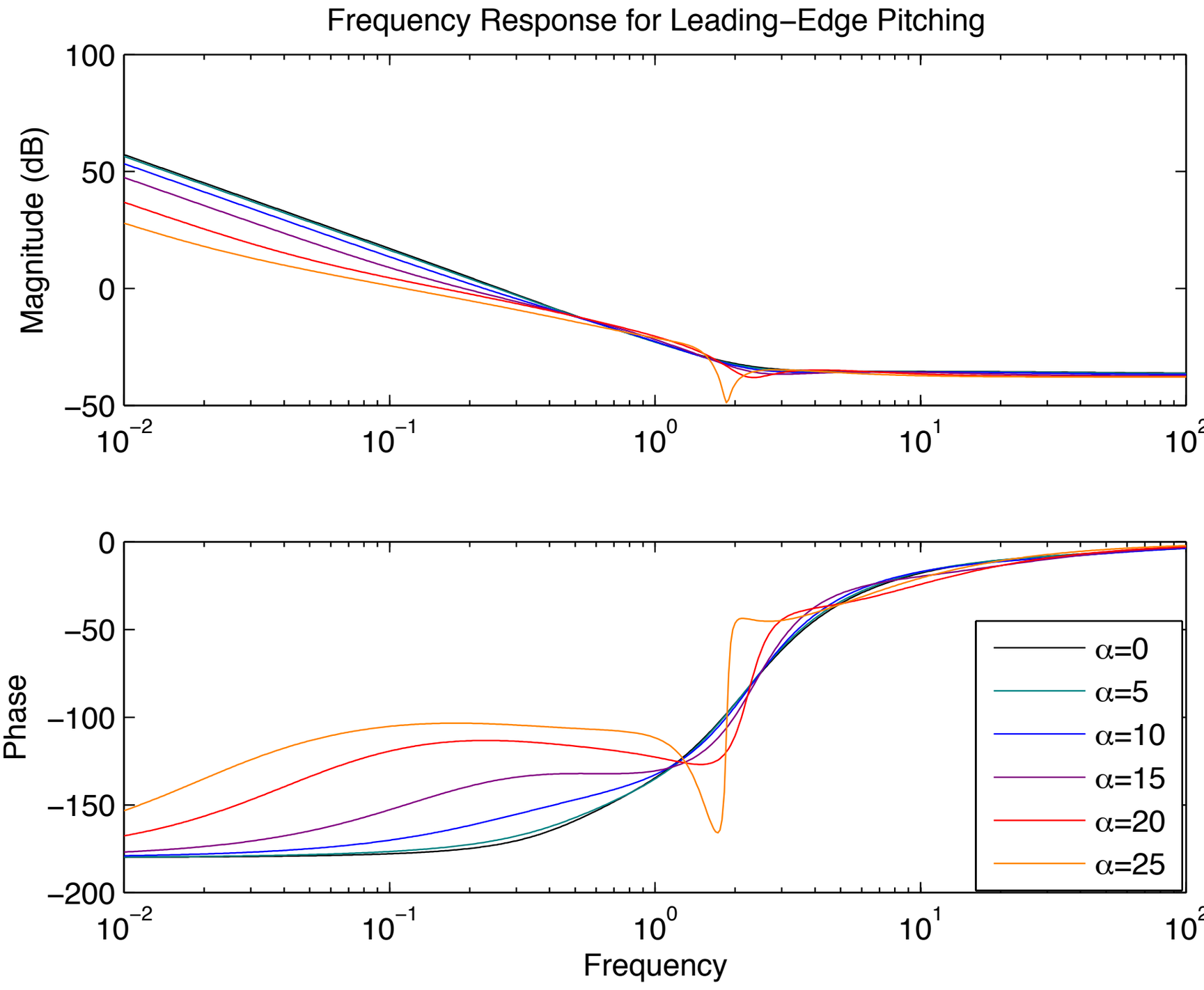

Poles and Zeros of ERA Models

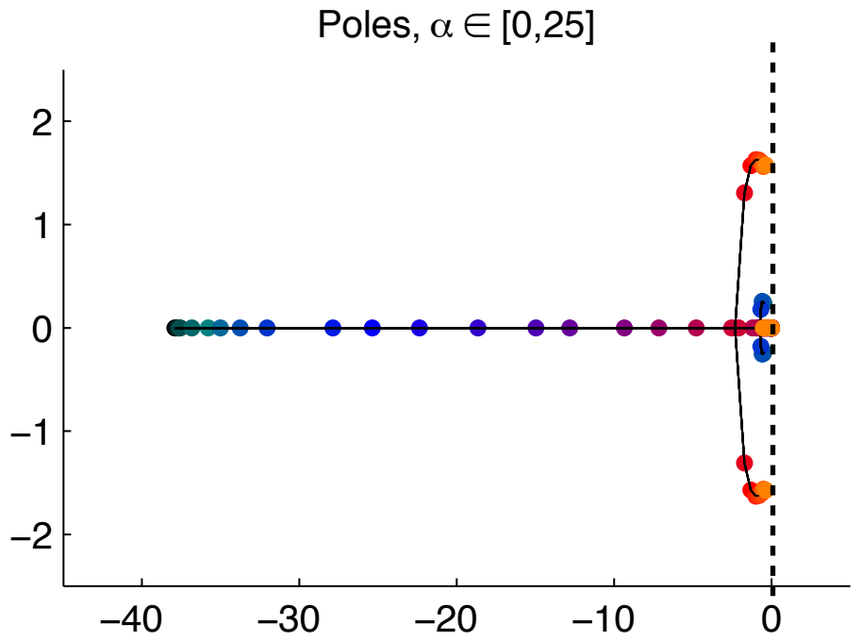

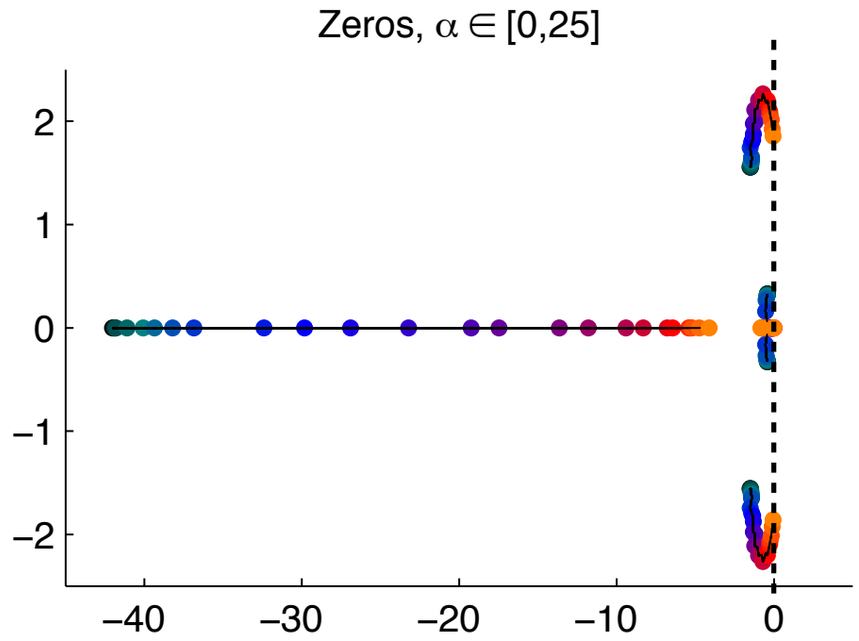

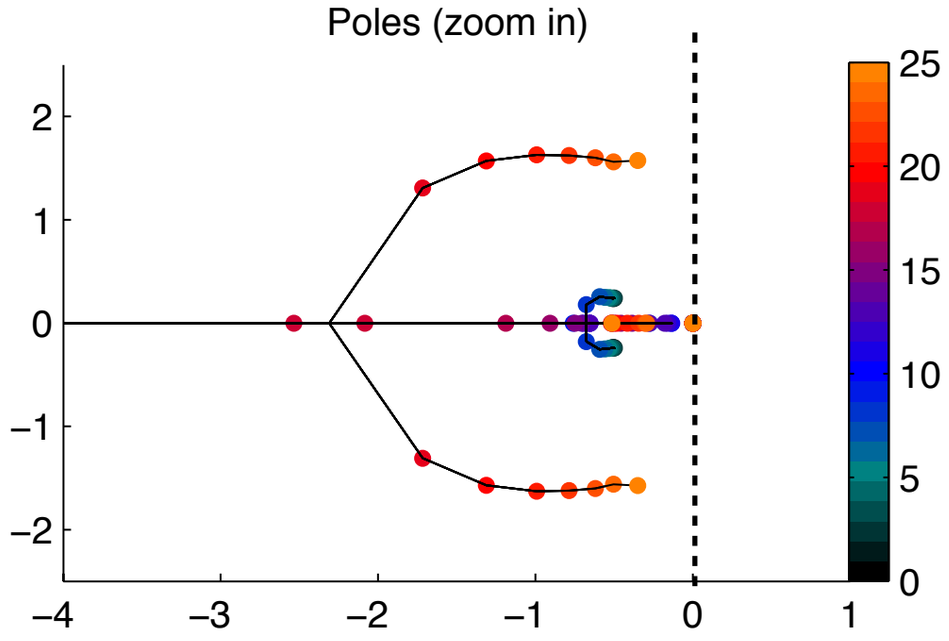

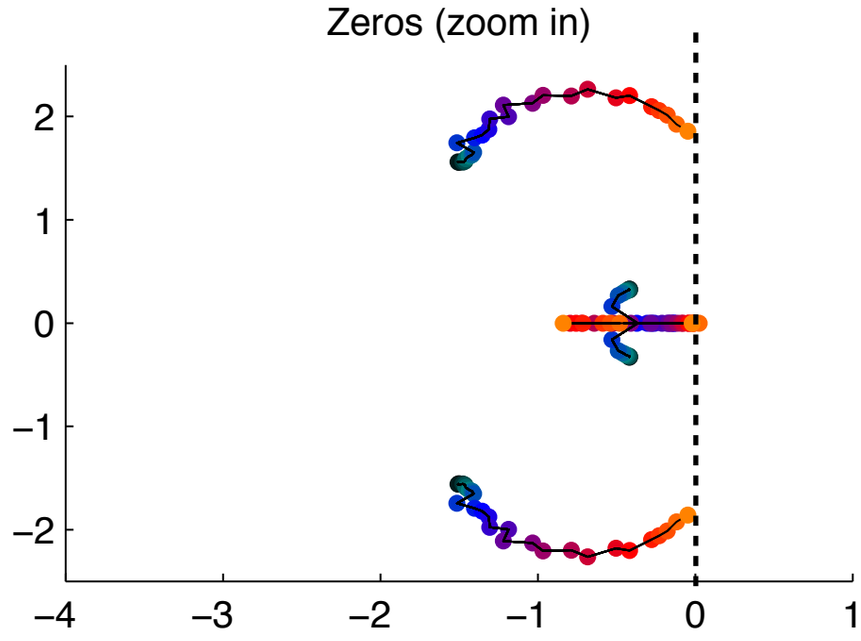

As angle of attack increases, pair of poles (and pair of zeros) march towards imaginary axis.

This is a good thing, because a Hopf bifurcation occurs at $\alpha_{\text{crit}} \approx 28^\circ$

Poles and Zeros of ERA Models

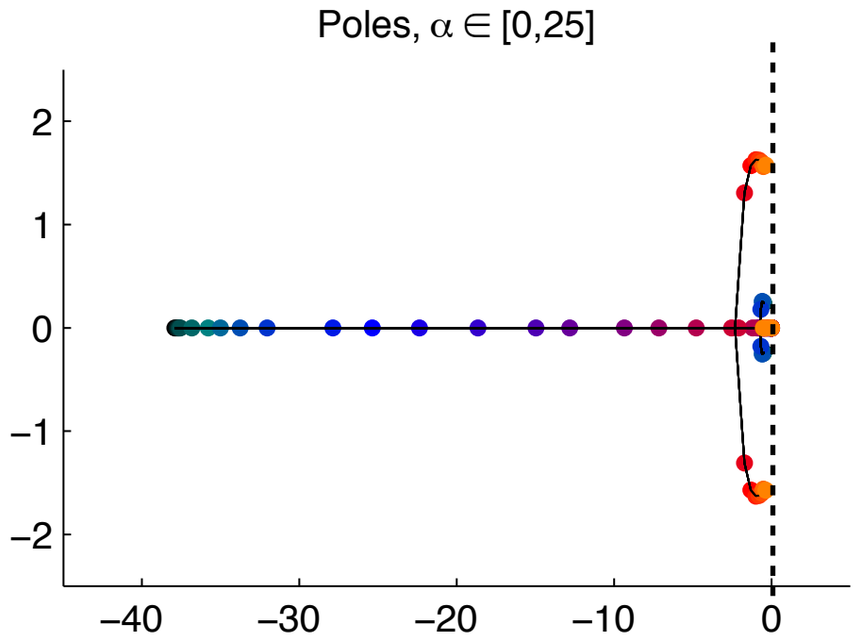

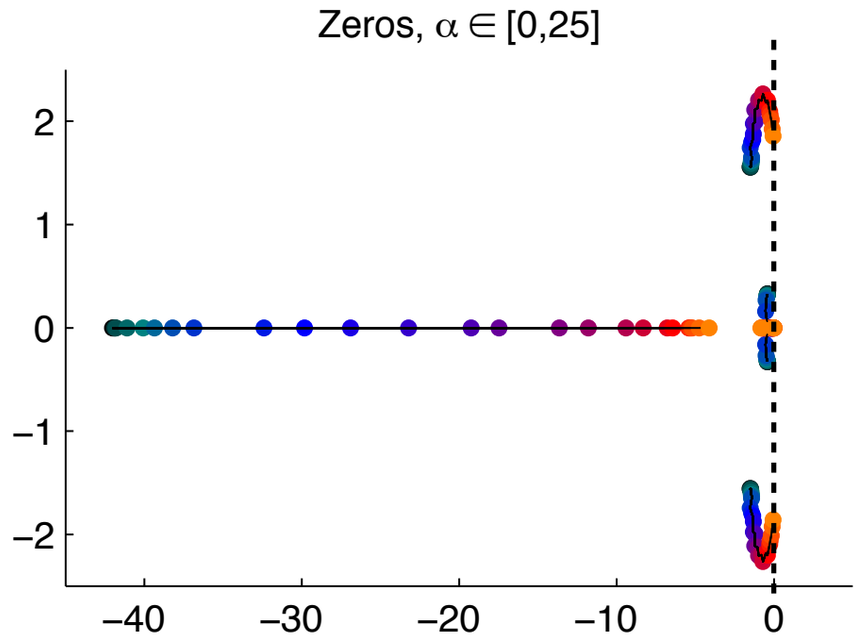

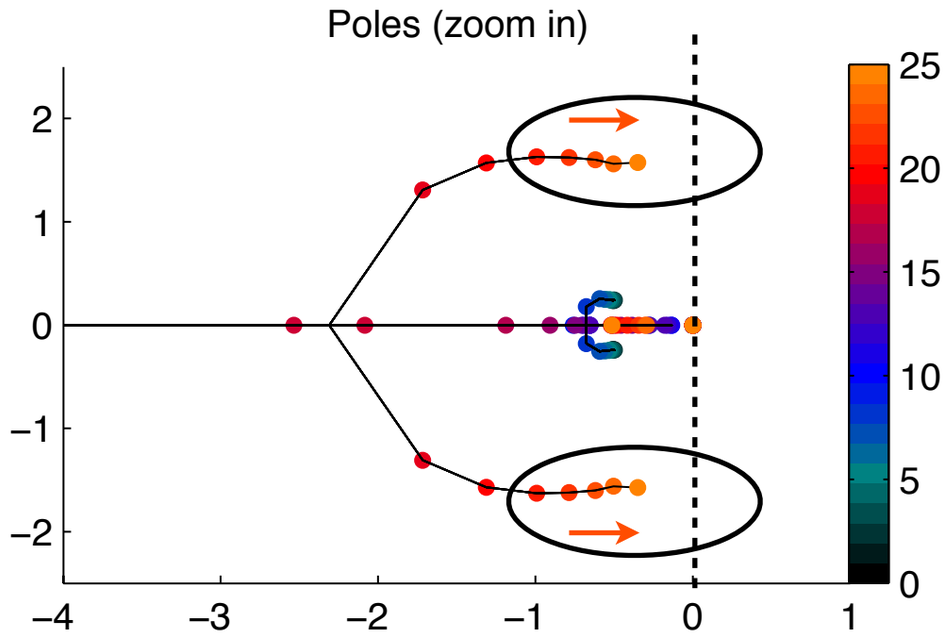

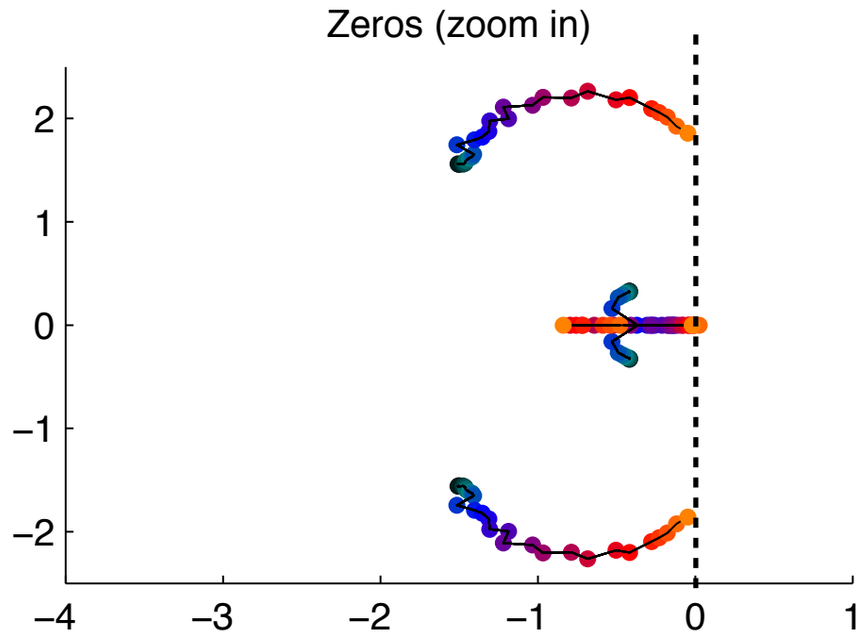

As angle of attack increases, pair of poles (and pair of zeros) march towards imaginary axis.

This is a good thing, because a Hopf bifurcation occurs at $\alpha_{\text{crit}} \approx 28^\circ$

Bode Plot of Model (-) vs Data (x)

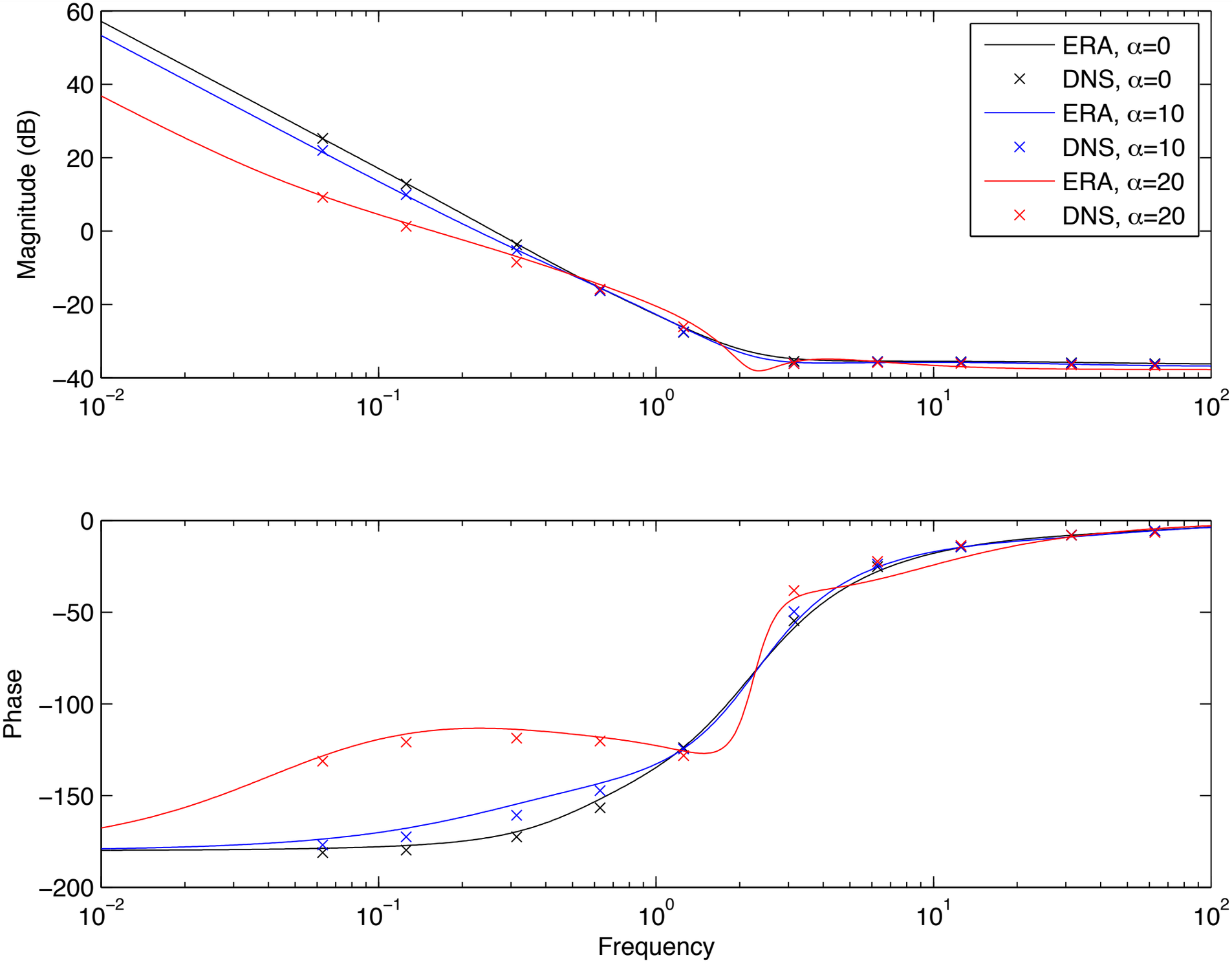

Direct numerical simulation confirms that local linearized models are accurate for small amplitude sinusoidal maneuvers

Large Amplitude Maneuver

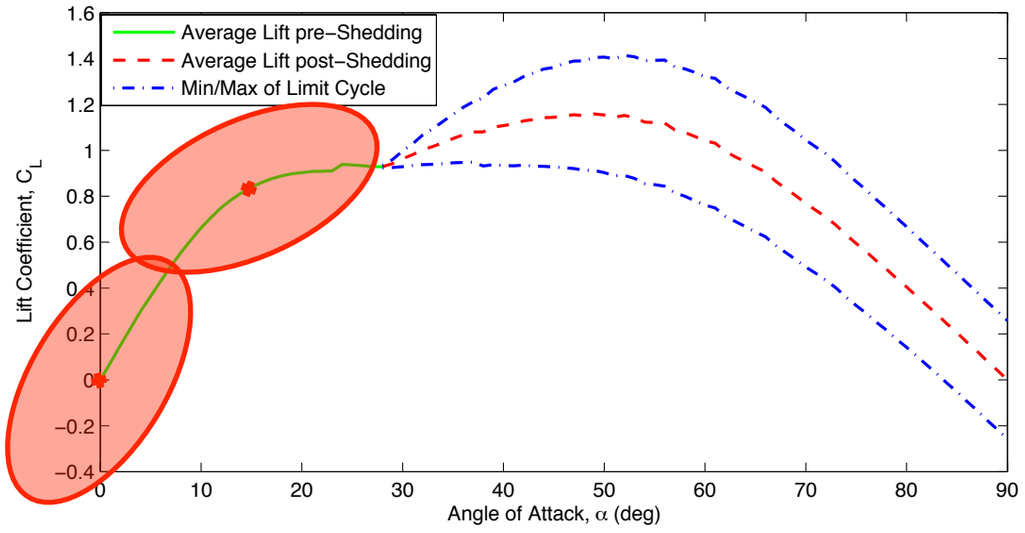

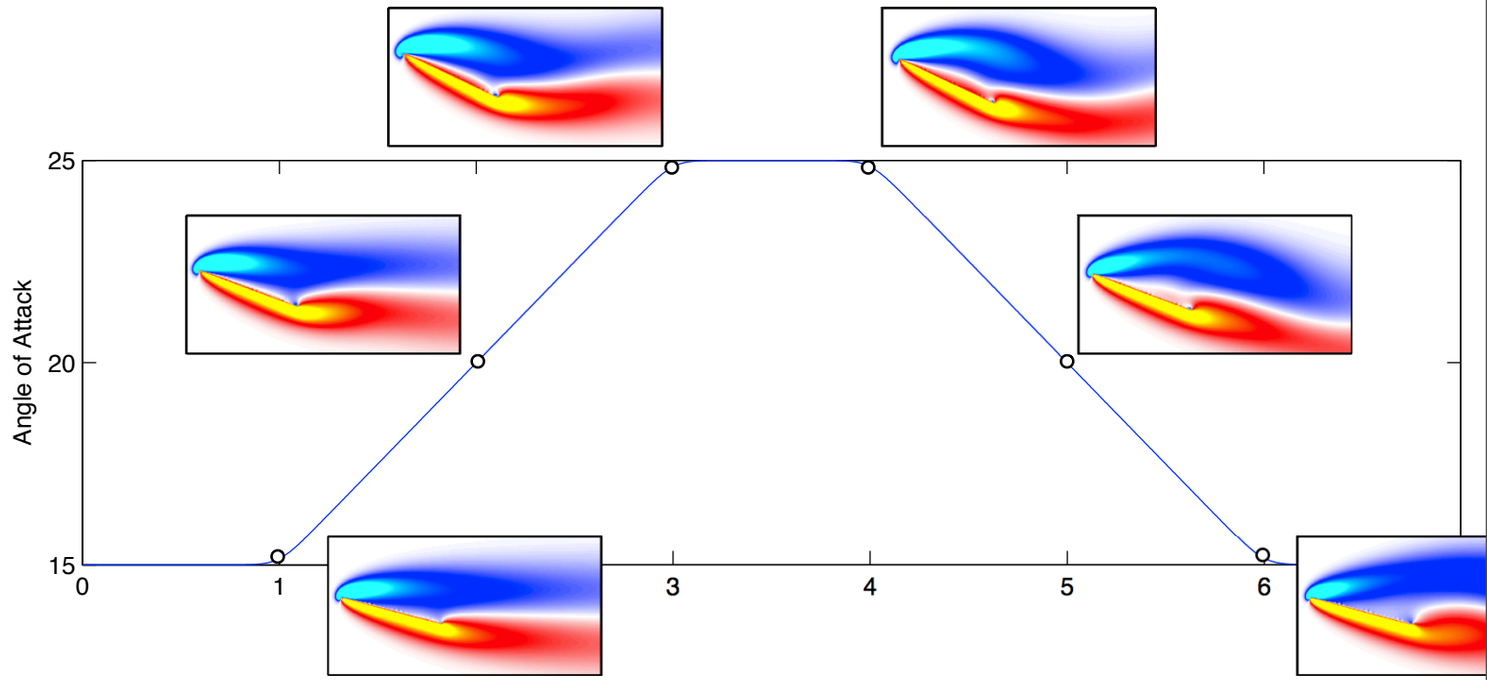

Compare models linearized at

$$\alpha = 0^\circ \quad \textbf{and} \quad \alpha = 15^\circ$$

For pitching maneuver with

$$\alpha \in [15^\circ, 25^\circ]$$

Model linearized at $\alpha = 15^\circ$

captures lift response more accurately

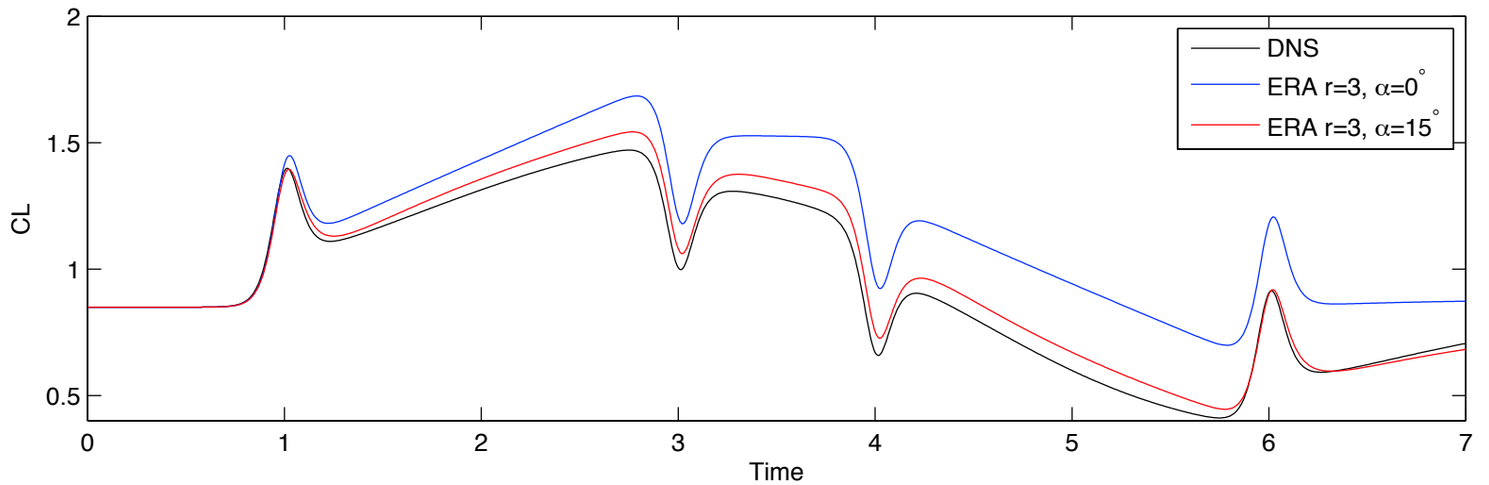

$$G(t) = \log\left[\frac{\cosh(a(t-t_1))\cosh(a(t-t_4))}{\cosh(a(t-t_2))\cosh(a(t-t_3))}\right] \qquad \alpha(t) = \alpha_0 + \alpha_{\max}\frac{G(t)}{\max(G(t))}$$

OL, Altman, Eldredge, Garmann, and Lian, 2010

Conclusions

Reduced order model based on indicial response at non-zero angle of attack

- Based on eigensystem realization algorithm (ERA)
- Models appear to capture dynamics near stall
- Locally linearized models outperform models linearized at $\alpha = 0^\circ$

Empirically determined Theodorsen model

- Theodorsen's C(k) may be approximated, or determined via experiments
- Models are cast into state-space representation
- Pitching about various points along chord is analyzed

Future Work:

- Combine models linearized at different angles of attack
- Add large amplitude effects such as gust disturbance or wake vortex

---

Wagner, 1925.

Theodorsen, 1935.

Leishman, 2006.

Brunton and Rowley, AIAA ASM 2009-2011

OL, Altman, Eldredge, Garmann, and Lian, 2010

Breuker, Abdalla, Milanese, and Marzocca, AIAA 2008.

Questions?

Steve Brunton & Clancy Rowley
Princeton University
FAA/JUP January 20, 2011